Journal of Medicinal Chemistry

ACS AuthorChoice

Article

pubs.acs.org/jmc

Terms of Use

Structure–Activity Relationship of 3,5-Diaryl-2-aminopyridine ALK2 Inhibitors Reveals Unaltered Binding Affinity for Fibrodysplasia Ossificans Progressiva Causing Mutants

Agustin H. Mohedas,[†,¶] You Wang,[‡,¶] Caroline E. Sanvitale,[§] Peter Canning,[§] Sungwoon Choi,[‡] Xuechao Xing,[‡] Alex N. Bullock,[§] Gregory D. Cuny,*[,‡,∥] and Paul B. Yu*[,⊥]

[†]Harvard–MIT Division of Health Sciences and Technology, Massachusetts Institute of Technology, 77 Massachusetts Avenue, Cambridge, Massachusetts 02139, United States

[‡]Laboratory for Drug Discovery in Neurodegeneration, Harvard NeuroDiscovery Center, Brigham and Women's Hospital and Harvard Medical School, 65 Landsdowne Street, Cambridge, Massachusetts 02139, United States

[§]Structural Genomics Consortium, University of Oxford, Oxford OX3 7DQ, United Kingdom

[∥]Department of Pharmacological and Pharmaceutical Sciences, University of Houston, Science and Research Building 2, Room 549A, Houston, Texas 77204, United States

[⊥]Department of Medicine, Cardiovascular Division, Brigham and Women's Hospital, 75 Francis Street, Boston, Massachusetts 02115, United States

Supporting Information

ABSTRACT: There are currently no effective therapies for fibrodysplasia ossificans progressiva (FOP), a debilitating and progressive heterotopic ossification disease caused by activating mutations of ACVR1 encoding the BMP type I receptor kinase ALK2. Recently, a subset of these same mutations of ACVR1 have been identified in diffuse intrinsic pontine glioma (DIPG) tumors. Here we describe the structure–activity relationship for a series of novel ALK2 inhibitors based on the 2-aminopyridine compound **K02288**. Several modifications increased potency in kinase, thermal shift, or cell-based assays of BMP signaling and transcription, as well as selectivity for ALK2 versus closely related BMP and TGF-β type I receptor kinases. Compounds in this series exhibited a wide range of in vitro cytotoxicity that was not correlated with potency or selectivity, suggesting mechanisms independent of BMP or TGF-β inhibition. The study also highlights a potent 2-methylpyridine derivative **10** (LDN-214117) with a high degree of selectivity for ALK2 and low cytotoxicity that could provide a template for preclinical development. Contrary to the notion that activating mutations of ALK2 might alter inhibitor efficacy due to potential conformational changes in the ATP-binding site, the compounds demonstrated consistent binding to a panel of mutant and wild-type ALK2 proteins. Thus, BMP inhibitors identified via activity against wild-type ALK2 signaling are likely to be of clinical relevance for the diverse ALK2 mutant proteins associated with FOP and DIPG.

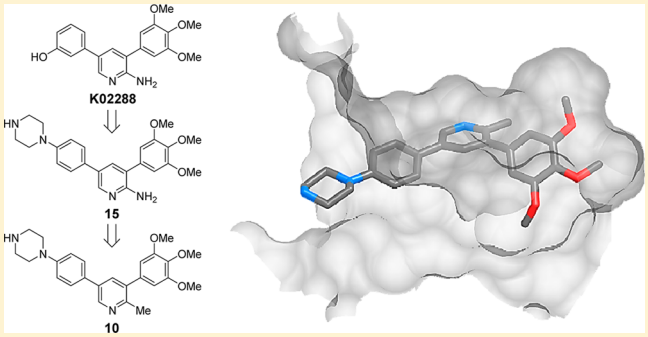

INTRODUCTION

Bone morphogenetic proteins (BMPs) are members of the transforming growth factor-beta (TGF-β) signaling family, which includes over 30 different ligands.[1] BMP signaling is essential for numerous processes, including cell fate determination, embryonic patterning, and iron homeostasis.[2,3] The BMP signaling cascade parallels that of TGF-β signaling. BMP ligand dimers bind to transmembrane receptor complexes consisting of two constitutively active type II receptor kinases (BMPRII, ACTRIIA, or ACTRIIB), which transphosphorylate and activate two type I receptor kinases (ALK1, ALK2, ALK3, or ALK6).[4] Activated type I receptors phosphorylate effector proteins (SMAD1/5/8) that complex with SMAD4, translocate to the nucleus, and activate BMP responsive genes such as the inhibitor of differentiation (Id) gene family. Functional and anatomic specificity of BMP signaling is regulated by the spatiotemporal expression of ligands and their cognate receptors as well as the expression of endogenous BMP antagonists such as noggin.[5,6]

Inappropriate BMP signaling has been shown to contribute to the pathophysiology of various disease processes.[7] One of the most striking examples of BMP signaling-related disease is seen in fibrodysplasia ossificans progressiva (FOP), a rare and disabling genetic disease affecting approximately 2500 people worldwide.[8] While individuals with the classical form of FOP

Received: November 24, 2013
Published: August 7, 2014

   dx.doi.org/10.1021/jm501177w | J. Med. Chem. 2014, 57, 7900–7915

are nearly normal at birth except for cervical and hallux joint deformities, during early life they develop progressive formation of endochondral bone in muscles, fascia, and ligaments, leading to severe immobility, pain, and premature mortality. A highly conserved gain-of-function mutation in the glycine−serine (GS) rich domain of the BMP type-I receptor ALK2 (c.617G>A; p.R206H) accounts for more than 98% of cases of classic FOP.[9,10] Several other FOP-causing gain-of-function mutations in both the GS and kinase domains of ALK2 have also been described in nonclassic or variant forms of FOP.[10−14]

Recently, several of the mutations identified in classic and nonclassic forms of FOP have been observed to arise in a proportion of tumors in diffuse intrinsic pontine glioma, a deadly childhood tumor also without effective therapies.[15−18] The consistency of this finding across diverse patient cohorts by several independent groups suggests an important role of somatic activating mutations of ACVR1 in this disease, however, the pathogenetic role of these mutant proteins is currently under investigation.

We and others have previously reported the discovery and development of small molecule inhibitors of BMP type-I receptors such as dorsomorphin, LDN-193189, LDN-212854, and DMH1, all of which are based on the pyrazolo[1,5-*a*]pyrimidine scaffold (Figure 1).[19−21] These compounds have

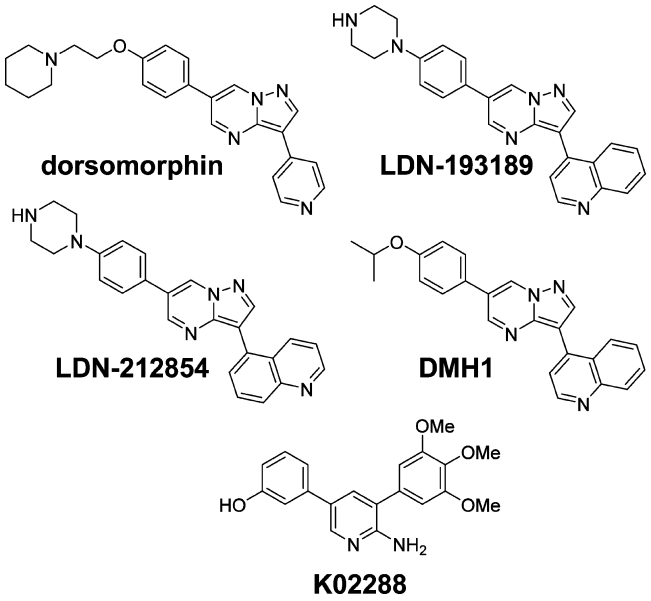

Figure 1. Previously described BMP inhibitors.

proven to be useful chemical reagents for the study of in vitro phenomenon, and several have demonstrated in vivo efficacy in a mouse model of FOP.[21,22] More recently we described a structurally distinct BMP type-I receptor inhibitor, **K02288**, which is based on a 2-aminopyridine scaffold and demonstrated greater kinome-wide selectivity than LDN-193189.[23] The 2-aminopyridine scaffold is also found in crizotinib, which was recently approved by the FDA for the treatment of nonsmall cell lung cancer in patients with activating mutations in the anaplastic lymphoma kinase.[24] Despite the high affinity and selectivity of **K02288** for BMP receptors in thermal shift and in vitro kinase assays, it has comparatively weak potency in cell-based assays.[21]

In this article, we describe a structure−activity relationship (SAR) study of **K02288** with respect to ALK2 binding affinity, BMP and TGF-β signaling inhibition in biochemical and cellular assays, selectivity, and cytotoxicity. These studies were pursued as part of an effort to elucidate the BMP type I receptor inhibitor pharmacophore, while producing a set of compounds with greater utility as physiologic probes. This SAR provides unique insights into features of 2-aminopyridine derivatives that are required for potent and selective inhibition of ALK2 versus closely related BMP and TGF-β receptors. We found that substitution of the 3-phenol with 4-phenylpiperazine greatly increased potency in cells, yielding a series of compounds more likely to be useful as probes of ALK2 function. These included a 2-methylpyridine derivative that exhibited potent and relatively selective inhibition of ALK2 activity in cell-based and in vitro kinase assays, high selectivity across the kinome, and low cytotoxicity. Additionally, we used this novel set of derivatives to demonstrate for the first time that FOP-causing mutations do not affect inhibitor binding affinity as compared to wild-type ALK2. This finding strongly suggests that ATP-competitive kinase inhibitors identified on the basis of their activity against endogenous BMP signaling, such as dorsomorphin and its derivatives, or by their affinity for wild-type ALK2, as in the case of **K02288**, will inhibit with equal potency the mutant $ALK2^{R206H}$ found in classical FOP as well as the other GS- and kinase-domain mutants of ALK2 that have been described in nonclassical or variant FOP or DIPG. These results describe a novel series of specific and potent probe compounds for the interrogation of BMP signaling that may have therapeutic potential for FOP and other diseases of maladaptive or inappropriate BMP signaling.

RESULTS AND DISCUSSION

Chemistry. A series of 2-amino-3-(3,4,5-trimethoxyphenyl)-pyridine derivatives were synthesized according to the procedures outlined in Scheme 1. Commercially available 2-amino-5-bromo-3-iodopyridine (**1**) was coupled with 3,4,5-trimethoxyphenylboronic acid under Suzuki reaction conditions to give **2** in 80% yield.[25−27] This intermediate was subjected to a second Suzuki reaction with a range of boronic acids to furnish the target compounds **3** in 40−85% yield.

Scheme 1. General Procedure for the Synthesis of 2-Amino-3-(3,4,5-trimethoxyphenyl)pyridine Derivatives[a]

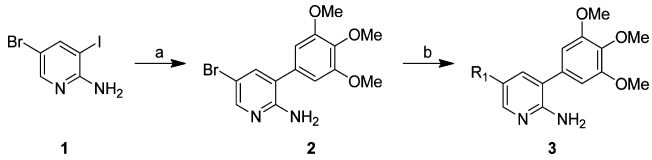

[a]Reagents and conditions: (a) 3,4,5-trimethoxyphenylboronic acid, MeCN/DMF, Na_2CO_3 (aqueous, 1 M), 10 mol % $Pd(PPh_3)_4$, 90 °C, 8 h, 80%; (b) arylboronic acid, DME, Na_2CO_3 (aqueous, 1 M), 10 mol %, $Pd(PPh_3)_4$, 90 °C, 8 h, 40−85%.

A variety of 2-substituted 3-aryl-5-(piperazinylphenyl)-pyridine derivatives were synthesized according to the method outlined in Scheme 2. An aryl group was first introduced at the 3-position of pyridine **1** or **4** via a Suzuki coupling to provide **5** in 65−85% yield. This was followed by a second Suzuki reaction using [(*N*-Boc)piperazin-1-yl]phenylboronic acid pinacol esters to generate **6**, which was deprotected using trifluoroacetic acid (TFA) in dichloromethane at room temperature to give amines **7**. Starting material **4** (R = NHMe or NMe_2) was prepared by reductive amination of **1** in

dx.doi.org/10.1021/jm501177w | J. Med. Chem. 2014, 57, 7900−7915

Scheme 2. General Procedure for the Synthesis of Various 2-Substituted 3-Aryl-5-(piperazinylphenyl)pyridine Derivatives[a]

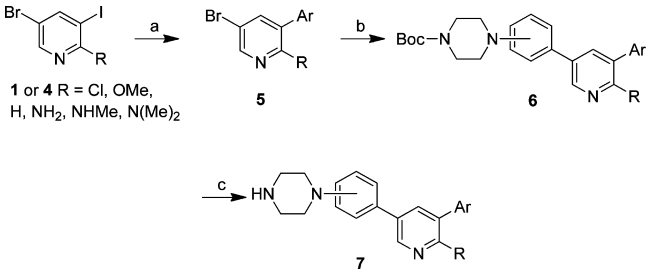

[a]Reagents and conditions: (a) arylboronic acid, MeCN/DMF, Na_2CO_3 (aqueous, 1 M), 10 mol % $Pd(PPh_3)_4$, 90 °C, 8 h, 65–85%; (b) [(*N*-Boc)piperazin-1-yl]phenylboronic acid pinacol ester, DME, Na_2CO_3 (aqueous, 1 M), 10 mol % $Pd(PPh_3)_4$, 90 °C, 8 h, 70–75%; (c) TFA, DCM, rt, 12 h, 100%.

dichloromethane using various amounts of paraformaldehyde in the presence of $NaBH(OAc)_3$.

3-Aryl-5-(4-piperazinylphenyl)pyridine derivatives containing a methyl substituent in the 2-position of the pyridine were prepared using the method outlined in Scheme 3. The 2-chloropyridine **8** was treated with trimethylboroxine in the presence of a palladium catalyst to generate 2-methylpyridine **9** in 90% yield.[28] The carbamate protecting group was again removed with TFA to generate **10**.

On the basis of several physiochemical properties, including calculated octanol–water partition coefficient (cLogP), distribution coefficient ($cLogD_{7.4}$), topological polar surface area (tPSA in Å^2), and number of hydrogen bond donors, acceptors (HBD and HBA) and rotatable bonds (Supporting Information, Table 1), the prepared compounds are predicted to be cell permeable and orally absorbed.[29,30]

SAR of Solvent Exposed Position. We previously demonstrated that **K02288** exhibits similar potency to LDN-193189 in biochemical kinase assays for inhibiting ALK2 and related BMP type I receptor kinases but was surprisingly less active in cell-based reporter assays using constitutively active BMP type I receptors.[21,23] We speculated the relatively weaker activity of **K02288** in cells might be due to poor solubility or impaired interactions with solvent water molecules that might be addressed via modifications in the solvent-exposed domain. We created six derivatives of **K02288** by modifying the 3-phenol substituent, which in the co-crystal structure of ALK2 occupied the solvent-exposed hydrophobic channel at the entrance of the ATP pocket (Supporting Information, Figure 1). Here, several functional groups were used as replacements of the 3-phenol (Figure 2a,b), chosen either to mimic hydrogen bonding of the phenol with Asp293 or to introduce an electropositive charge (e.g., a protonated amine) to mediate an ionic interaction with Asp293, thus maintaining a potentially important interaction. To gain insight into the potency and selectivity for BMP vs TGF-β signaling, derivatives were tested for their ability to bind BMP type I receptor ALK2 and TGF-β type I receptor ALK5, using an in vitro thermal shift kinase assay (Figure 2c). This type of assay has been previously shown by us and others to be highly predictive of biochemical kinase inhibition activity,[31] which was also measured in a selected subset of the derivatives (Figures 2–5). Tm shift data were found to correlate highly ($r^2 \geq 0.8$) with biochemical inhibition data (Supporting Information, Figure 2). To assess the potency and selectivity of these compounds in cells, inhibition of BMP6-induced transcriptional activity (BRE-Luciferase) and TGF-β1-induced transcriptional activity (CAGA-Luciferase) was measured for each of the compounds (Figure 2c), using cell lines (C2C12 for BMP6 and HEK293T for TGF-β1) previously shown to express a complement of BMP or TGF-β receptors required for ligand-mediated signaling.[32] In general, the magnitude of ΔT_m for ALK2 and ALK5 correlated inversely with the log IC_{50} for inhibition of BMP and TGF-β-induced transcriptional activity (Figure 1d) but with some minor exceptions. Notably, **K02288** exhibited a large thermal shift for ALK2 kinase protein (ΔT_m = 13.2 °C), consistent with potent inhibition of ALK2 activity by biochemical assay (IC_{50} = 34 nM) but was substantially weaker in the cell-based assay of BMP6 activity (IC_{50} = 421 nM, Figure 2c). Of the variants at the 3-phenol position, compound **13** exhibited the best in vitro inhibition of ALK2, whereas compound **15** demonstrated the best cell-based activity. The occasional discordance between biochemical (ΔT_m and enzymatic) and functional assays (ligand-induced transcription) highlighted the need for multiple assays in an SAR aimed at identifying physiologic probes with useful potency and selectivity.

In addition to altering potency, modifications to the solvent-exposed 3-phenol showed significant alterations in selectivity. Replacing 3-phenol with 4-phenol (**11**) increased potency against BMP6 signaling by ~20-fold compared to **K02288** while retaining a modest degree of selectivity for BMP6 versus TGF-β1 signaling (28-fold, Figure 2c). Adding a 3-methoxy group to the 4-phenol (**12**) reduced BMP6 inhibition modestly, with similar selectivity. Replacing the 3-phenol with a bioisosteric methylsulfonamide (**13**) improved BMP6 inhibition compared to **K02288** but decreased selectivity. The largest increase in potency occurred with the replacement of the 3-phenol with 3- or 4-phenylpiperazine, as previously done with LDN-193189, likely due to the increased polarity of this

Scheme 3. Synthesis of a 2-Methyl 3-Aryl-5-(4-piperazinylphenyl)pyridine Derivatives[a]

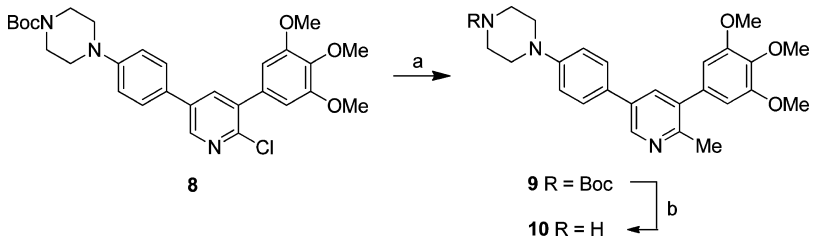

[a]Reagents and conditions: (a) trimethylboroxine, 1,4-dioxane, K_2CO_3 (2 equiv), 20 mol % $Pd(PPh_3)_4$, 110 °C, 8 h, 90%; (b) TFA, DCM, rt, 12 h, 100%.

dx.doi.org/10.1021/jm501177w | J. Med. Chem. 2014, 57, 7900–7915

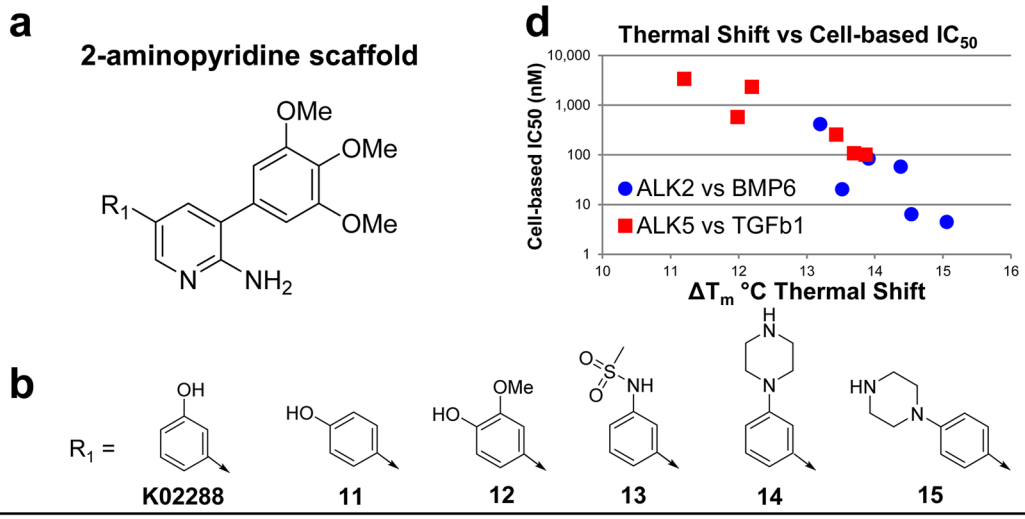

c	ALK2 ΔT_m(°C)	ALK5 ΔT_m(°C)	ΔT_m Diff.	ALK2 IC_{50} (nM)	ALK5 IC_{50} (nM)	BMP6 IC_{50} (nM)	TGFβ1 IC_{50} (nM)	Fold Select.
K02288	13.2	11.2	2.0	35	280	420 ± 170	3,400 ± 500	8
11	13.5	12.0	1.5	nd	nd	20 ± 1	580 ± 50	28
12	13.9	12.2	1.7	nd	nd	90 ± 30	2,300 ± 300	28
13	14.4	13.4	0.9	6	180	60 ± 10	260 ± 20	4
14	14.5	13.7	0.8	17	49	6 ± 1	110 ± 20	17
15	15.1	13.9	1.2	10	186	4 ± 1	100 ± 10	23

Figure 2. Potency and selectivity of **K02288** derivatives based on thermal shift, biochemical kinase activity, and ligand induced transcriptional activity assays. (a) The 2-aminopyridine scaffold of **K02288**. (b) Modifications to the solvent exposed domain (R_1) of **K02288**. (c) Thermal shift (ΔT_m), biochemical enzymatic inhibition (IC_{50}) for ALK2 and ALK5 kinase proteins, and inhibition of cell-based BMP6 and TGF-β1-induced transcriptional activity (IC_{50}) by **K02288** derivative compounds (nd = not determined). (d) Correlation of thermal shift and cell-based BMP/TGF-β inhibition assays.

substituent resulting in both improved inhibitor aqueous solubility and increased enthalpic interactions with solvent water molecules.[19] Compounds **14** and **15** demonstrated 70–100-fold increases in BMP6 inhibition (IC_{50} = 6 nM, and 4 nM) compared to **K02288**, with modest improvements in selectivity. Compound **15** is structurally similar to previously disclosed aminopyridine inhibitors of interleukin-2-inducible T-cell kinase (ITK) and pyridine benzamide inhibitors of protein kinase D (PKD).[33,34] To further investigate the type I receptor selectivity of **15**, cells were transfected with adenoviruses expressing constitutively active BMP type I receptors (caALK1, caALK2, and caALK3) and constitutively active activin or TGF-β type I receptors (caALK4 and caALK5) in low serum conditions and in the absence of exogenous ligand (Supporting Information, Figure 3). Derivative **15** was most potent against BMP receptors caALK2 and caALK3 with IC_{50} measurements of ~3.5 nM, whereas the activin/TGF-β type I receptors and caALK1 were inhibited with with an IC_{50} measurements of ~20 nM, with nearly complete extinction of BMP and TGF-β type I receptor signaling at approximately 250 nM. Taken together, these data demonstrate that replacing the 3-phenol in the solvent exposed region of **K02288** with 4-phenylpiperazine dramatically improved its potency in cells but with relatively poor selectivity for BMP versus TGF-β signaling. These results prompted us to explore structural variants at other positions that might refine selectivity while retaining gains in potency afforded by modification of the solvent-exposed 3-phenol with 4-phenylpiperazine in **15**.

SAR of Hydrophobic Pocket Position. Further modifications of potent compound **15** were performed to develop an SAR for the 3,4,5-trimethoxyphenyl group (R_2) (Figure 3a,b) to identify the role of each methoxy group on potency and selectivity. The trimethoxyphenyl group has previously been shown to interact with the hydrophobic back pocket in ALK2 where it forms water-mediated hydrogen bonds with the catalytic lysine residue (K235) (Supporting Information, Figure 1). Compounds were again profiled in thermal shift, biochemical enzyme inhibition, and cell-based luciferase reporter assays (Figure 3b,c).

Removal of any of the methoxy groups resulted in a significant decrease in BMP inhibition. However, particular methoxy groups were more crucial than others. For example, removing one of the 3-methoxy groups (**16**) resulted in a 35-fold loss in potency compared to **15**, although selectivity for BMP6 inhibition versus TGF-β increased. Removing the 4-methoxy group (**17**) decreased activity 10-fold but did not improve selectivity. Combining these changes (**18**) demonstrated that the 4-methoxy group contributed less significantly to BMP6 inhibition as compared to either *meta*-methoxy group. As expected, removal of both *meta*-methoxy groups, while

dx.doi.org/10.1021/jm501177w | J. Med. Chem. 2014, 57, 7900–7915

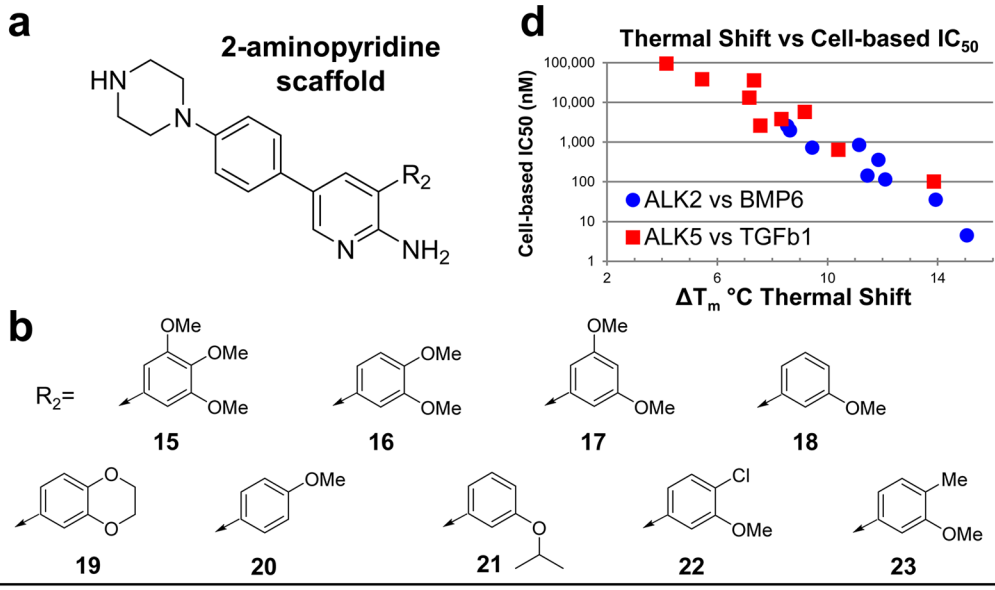

c	ALK2 ΔT_m(°C)	ALK5 ΔT_m(°C)	ΔT_m Diff.	ALK2 IC_{50} (nM)	ALK5 IC_{50} (nM)	BMP6 IC_{50} (nM)	TGFβ1 IC_{50} (nM)	Fold Select.
15	15.1	13.9	1.2	10	190	4 ± 1	100 ± 10	23
16	11.5	7.2	4.3	23	6,900	140 ± 30	13,100 ± 1,000	92
17	13.9	10.4	3.5	14	1,000	40 ± 10	650 ± 80	18
18	12.1	8.3	3.8	86	12,300	110 ± 10	3,800 ± 200	33
19	9.5	5.5	4.0	1,870	15,000	730 ± 100	38,000 ± 8,500	53
20	8.6	4.2	4.5	nd	nd	1,900 ± 900	95,000 ± 23,000	48
21	8.5	7.6	1.0	790	1,400	2,500 ± 90	2,600 ± 400	1
22	11.9	9.2	2.7	63	1,910	360 ± 10	5,800 ± 600	16
23	11.2	7.3	3.8	110	21,000	840 ± 120	35,500 ± 13,000	42

Figure 3. Potency and selectivity of compound **15** derivatives based on thermal shift, biochemical kinase activity, and ligand induced transcriptional activity assays. (a) The 2-aminopyridine scaffold of **15**. (b) Modifications to the ATP-binding pocket hydrophobic domain (R_2) of compound **15**. (c) Thermal shift (ΔT_m), biochemical enzymatic inhibition (IC_{50}) for ALK2 and ALK5 kinase proteins, and inhibition of cell-based BMP6 and TGF-β1-induced transcriptional activity (IC_{50}) by compound **15** derivatives (nd = not determined). (d) Correlation of thermal shift and cell-based BMP/TGF-β inhibition assays.

retaining the *para*-methoxy group (**20**) drastically reduced potency by almost 500-fold. Incorporating the 3,4-dimethoxy groups into a benzo-1,4-dioxane (**19**) resulted in decreased activity compared to **16**, perhaps reflecting disruption of the hydrogen bond with ALK2 residue K235. In addition, increasing the steric bulk of the 3-alkoxy group (**21**) or replacing the 4-methoxy with a chlorine (**22**) or a methyl (**23**) were also not productive. In conclusion, of the compounds studied the 3,4,5-trimethoxphenyl group resulted in the best balance between BMP6 inhibition and selectivity over TGF-β. This is likely due to its greater molecular volume for occupying the hydrophobic pocket in ALK2 while retaining hydrogen bond acceptors in the meta-positions of the phenyl ring. Future studies will seek to optimize binding in the hydrophobic pocket by replacing the 3,4,5-trimethoxyphenyl entirely with a diverse set of aryl and heteroaryl moieties.

SAR of Hinge Binding Position. To further explore the SAR of **15**, we modified the primary amine residue of the 2-aminopyridine (R_3, Figure 4a,b), a region that was previously shown to interact with the hinge region of the ALK2 kinase domain. Here, the amine was within hydrogen bonding distance to the backbone carbonyl of H284, as well as the gatekeeper residue T283 of ALK2 (Supporting Information, Figure 1). Both residues are changed in ALK5 (D281 and S280, respectively). Secondary and tertiary amines such as **24** and **25**, respectively, exhibited reduced potency in both the thermal shift and cell-based assays. Similarly, **28**, in which the primary amine is replaced with a methoxy substituent, exhibited decreased potency, suggesting that bulky substituents are not well tolerated at this position. Notably, these compounds exhibited negligible thermal shift despite detectable albeit low activity in cell-based assays (Figure 4c). Despite the high degree of correlation between the thermal shift and cell-based assays (Supporting Information, Figure 4), compounds that exhibit very low ΔT_m may exhibit measurable inhibition in cells at moderately high concentrations, potentially due to cytotoxicity

dx.doi.org/10.1021/jm501177w | J. Med. Chem. 2014, 57, 7900−7915

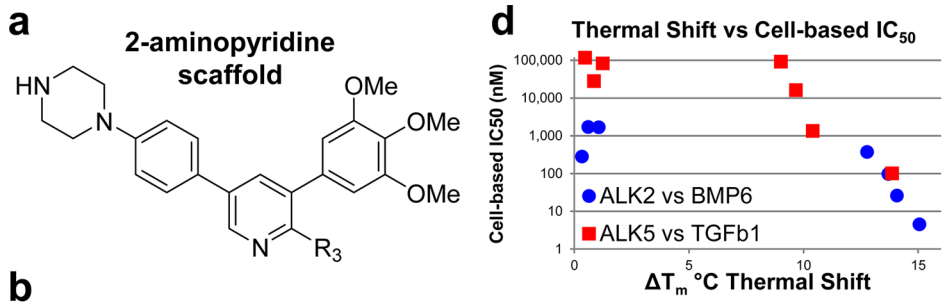

b

R_3 =	NH_2	NHMe	NMe_2	H	Cl	Me	OMe
	15	**24**	**25**	**26**	**27**	**10**	**28**

c	ALK2 ΔT_m(°C)	ALK5 ΔT_m(°C)	ΔT_m Diff.	ALK2 IC_{50} (nM)	ALK5 IC_{50} (nM)	BMP6 IC_{50} (nM)	TGFβ1 IC_{50} (nM)	Fold Select.
15	15.1	13.9	1.2	10	190	4 ± 1	100 ± 10	23
24	0.3	0.9	-0.5	nd	nd	280 ± 60	28,000 ± 5,300	99
25	0.6	0.5	0.1	nd	nd	1,700 ± 400	115,000 ± 30,000	68
26	14.1	10.4	3.7	15	240	30 ± 2	1,300 ± 200	51
27	12.8	9.0	3.8	nd	nd	370 ± 60	90,000 ± 34,000	244
10 (LDN-214117)	13.7	9.7	4.0	24	3,000	100 ± 1	16,000 ± 4,000	164
28	1.1	1.2	0.1	nd	nd	1,700 ± 300	82,000 ± 1,200	48

Figure 4. Potency and selectivity of **K02288** derivatives based on thermal shift, biochemical kinase activity, and ligand induced transcriptional activity assays. (a) The 2-aminopyridine scaffold of **15**. (b) Modifications to the primary amine kinase hinge binding domain (R_3) of compound **15**. (c) Thermal shift (ΔT_m), biochemical enzymatic inhibition (IC_{50}) for ALK2 and ALK5 kinase proteins, and inhibition of cell-based BMP6 and TGF-β1-induced transcriptional activity (IC_{50}) by compound **15** derivatives (nd = not determined). (d) Correlation of thermal shift and cell-based BMP/TGF-β inhibition assays.

at high concentrations (>50 μM, Supporting Information, Figure 5). Replacing the primary amine with hydrogen (**26**) resulted in only a modest decline in potency and significantly increased selectivity for BMP6 versus TGF-β signaling, suggesting that the primary amine hydrogen bond to the hinge backbone is more critical for binding to ALK5 (D281) than ALK2 (H284). Finally, we used two other small substituents, e.g., chlorine (**27**) and methyl (**10**) groups to explore the possibility that ALK2 is less sensitive than ALK5 to substituents at this position. Although both compounds lost potency relative to **26**, there was a significant increase in selectivity for BMP over TGF-β signaling, with both showing greater than 150-fold selectivity in cell-based assays. In particular, **10** remained relatively potent with a biochemical IC_{50} of 24 nM for ALK2, a cell-based IC_{50} for BMP6 of approximately 100 nM, and 164-fold selectivity for BMP6 versus TGF-β1. The activities of compounds **15**, **26**, and **10** in the thermal shift kinase assay as well as two different cell-based assays (ligand induced transcription and constitutively active type I receptor transcriptional activity) are summarized in Supporting Information, Table 2. In each of the various assays, compound **10** (LDN-214117) exhibited improved selectivity for ALK2 versus ALK5 signaling, consistent with a high degree of selectivity for BMP versus TGF-β signaling. In fact, when the activity of **10** was measured against closely related BMP type I receptors ALK1−3 via kinase assays, it appeared to inhibit ALK2 more potently than ALK3 by more than 40-fold (Figure 6a), a degree of selectivity which rivals previously reported compound LDN-212854.[21] We tested whether or not compounds with improved receptor selectivity such as **10** or **26** might also exhibit more selective inhibition of BMP ligands. We found that both of these compounds impacted the transcriptional activity of a BMP-responsive luciferase reporter (BRE-Luc) in response to BMP6, a known ALK2 ligand, more potently than that of BMP2 or BMP4, classic ligands of ALK3 (Figure 6b−d).[35] In fact, compound **10** inhibited BMP6 preferentially to BMP2 and BMP4 by approximately 10-fold, whereas **K02288** and compound **15** inhibited BMP2, -4, and -6 with equal potency. These data support the concept that increased selectivity of **10** and **26** for ALK2 translates into increased selectivity for the activity of ligands which signal primarily through ALK2, a class which include BMP6 and BMP7.[36] These results further highlight that the 2-position of the pyridine in the **K02288** series can be exploited to achieve reasonably potent and highly selective BMP inhibitors, presumably via optimization of hinge domain interactions.

*SAR of **K02288** and LDN-193189 Hybrid Molecules.* We previously described a highly selective pyrazolo[1,5-*a*]-pyrimidine based BMP type I receptor kinase inhibitor LDN-212854 that exhibited biased activity for ALK2. This selectivity was achieved by a 5-quinoline moiety that interacts with the same hydrophobic pocket as the 3,4,5-trimethoxy group of **K02288**. With this in mind, we synthesized several derivatives of **15** that replaced the 3,4,5-trimethoxyphenyl with 4- or 5-

dx.doi.org/10.1021/jm501177w | J. Med. Chem. 2014, 57, 7900−7915

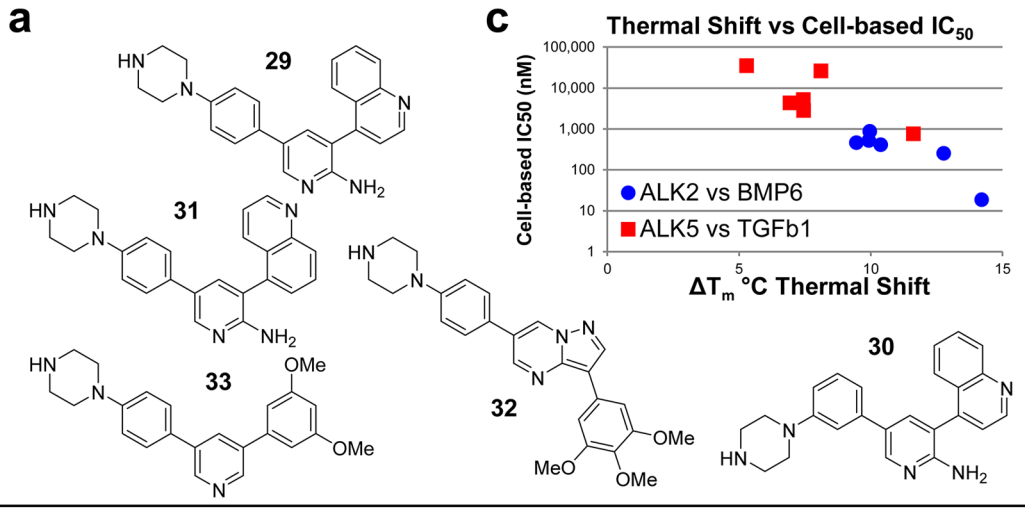

b	ALK2 ΔT_m(°C)	ALK5 ΔT_m(°C)	ΔT_m Diff.	ALK2 IC_{50} (nM)	ALK5 IC_{50} (nM)	BMP6 IC_{50} (nM)	TGFβ1 IC_{50} (nM)	Fold Select.
29	10.4	6.9	3.4	120	21,000	410 ± 50	4,300 ± 300	11
30	9.9	7.4	2.5	110	5,000	520 ± 60	2,800 ± 300	5
31	9.4	5.3	4.2	270	99,000	470 ± 60	34,800 ± 9,000	75
32	14.2	11.6	2.6	10	30	20 ± 2	760 ± 80	41
33	12.8	8.1	4.7	nd	nd	260 ± 40	26,000 ± 4,000	102

Figure 5. Potency and selectivity of **K02288** derivatives based on thermal shift, biochemical kinase activity, and ligand induced transcriptional activity assays. (a) Structure of hybrid derivative molecules. (b) Thermal shift (ΔT_m), biochemical enzymatic inhibition (IC_{50}) for ALK2 and ALK5 kinase proteins, and inhibition of cell-based BMP6 and TGF-β1-induced transcriptional activity (IC_{50}) by hybrid molecules (nd = not determined). (c) Correlation of thermal shift and cell-based BMP/TGF-β inhibition assays.

quinolines (Figure 5a). As expected, the 5-quinoline (**31**) demonstrated substantially increased selectivity for BMP versus TGF-β inhibition (Figure 5b). However, all of these compounds were substantially less potent than **15**. Modeling of these 5-quinoline substituted compounds in the ATP-binding pocket suggested that binding to the kinase hinge by the 2-aminopyridine scaffold may constrain the quinoline moiety to a suboptimal position as compared to the pyrazolo[1,5*a*]pyrimidine scaffolds (Supporting Information, Figure 6). Conversely, replacing the 5-quinoline of LDN-212854 with the 3,4,5-trimethoxyphenyl of **K02288** yielded **32** that demonstrated potent BMP6 inhibitory activity but with less selectivity. Finally, hypothesizing that two individual changes yielding improvements in selectivity might synergize, we combined the substitutions of the 2-amino group with hydrogen and the 3,5-dimethoxy group found in **26** and **17** to yield **33**. Although this molecule demonstrated improved selectivity it had considerably less potency.

Kinome-Wide Selectivity. We previously reported the kinome-wide selectivity for both **K02288** and LDN-193189, showing that **K02288** has a more selective profile with fewer off-target kinases inhibited at low (0.1 μM) and high (1.0 μM) concentrations.[21,23] We sought to determine the kinome-wide selectivity of **K02288** derivative compounds **10** (LDN-214117) and **15**, via enzymatic kinase profiling of approximately 200 kinases, summarized in the kinome dendrogram shown in Figure 7. The kinase most highly inhibited by compound **10** (LDN-214117) was ALK2, followed by TNIK, RIPK2, and ABL1 (detailed results of kinome profiling provided in Supporting Information, Table 3). Although less potent than **15**, compound **10** (LDN-214117) demonstrated significant improvement in selectivity across the kinome. At 100 nM and 1 μM, compound **10** inhibited only 0.5% and 3.6% of kinases profiled by more than 50%, whereas compound **15** inhibited 2.1% and 14.4% of kinases profiled, respectively. Compound **10** thus exhibited improved kinome selectivity than that previously reported for LDN-193189, LDN-212854, or **K02288**.[21,23]

FOP Mutations and Inhibitor Binding. The majority of individuals with FOP harbor the R206H germline mutation affecting the glycine−serine (GS-) rich regulatory domain of ALK2.[9,37−39] While several of the other known FOP-causing mutations also involve residues of the GS-domain (i.e., L196P, R202I, and Q207E), several affect important regulatory sites within the kinase domain (i.e., G328E/R/W, R258S, G356D, and R375P).[11−14,23,40] A subset of both GS-domain and kinase domain mutations associated with FOP have also been found to arise somatically in 20−30% of DIPG tumor tissues, frequently in combination with mutations affecting the loci encoding histone H3.1[15−18]

We and others have shown that much of the enhanced cellular activity of various FOP-causing ALK2 mutants is attributable to differential regulation of the signaling pathway, i.e., impaired interactions with kinase regulatory protein FKBP12, and differential basal versus ligand-induced signaling activity.[40,41] However, there is the possibility that ALK2 mutants have intrinsic differences in their enzymatic function,

dx.doi.org/10.1021/jm501177w | J. Med. Chem. 2014, 57, 7900−7915

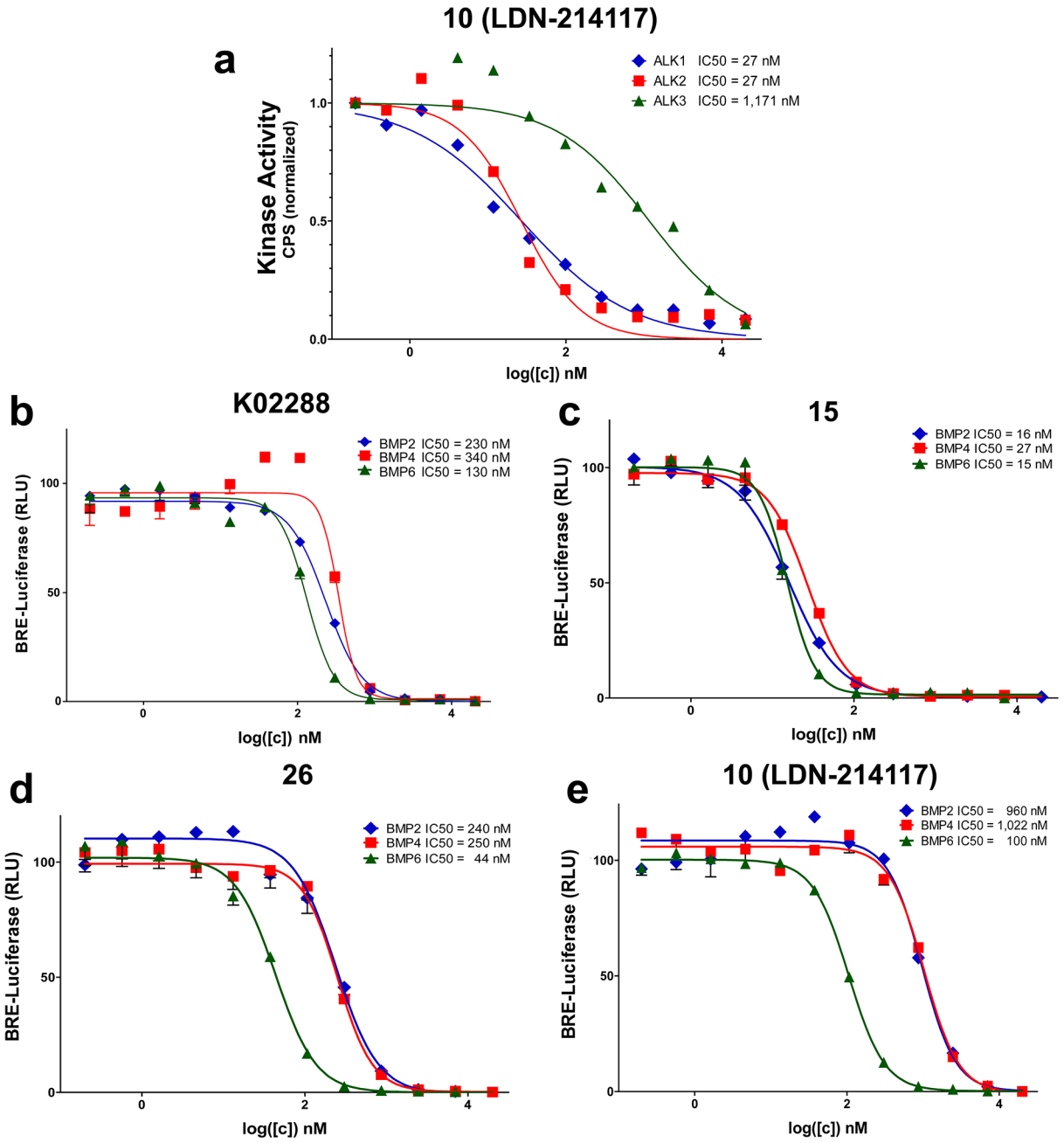

Figure 6. LDN-214117 exhibits selectivity for ALK2-mediated BMP signaling. (a) **10** (LDN-214117) demonstrates selective inhibition of ALK2 and ALK1 in preference to ALK3 kinase activity. (b) In a cell-based assay measuring BMP-mediated transcription (BRE-Luciferase), **K02288** (b) and **15** (c) exhibit relatively limited selectivity for diverse BMP ligands, whereas **26** (d) and **10** (e) exhibit relatively selective inhibition of BMP6 versus BMP2 or BMP4, consistent with selective inhibition of ALK2- versus ALK3-mediated signaling, respectively.

which could manifest as differences in affinity for ATP and altered K_m, with implications for their cellular activity and susceptibility to inhibitors. We tested this directly by measuring the K_m for ATP of wild-type ALK2 and four FOP-causing ALK2 mutants (L196P, Q207E, G328E, and R258S). The K_m values for wild type and mutant ALK2 were between 16 and 48 μM (Supporting Information, Table 4). Importantly, none of the FOP-causing mutants exhibited enhanced affinity for ATP as compared with wild-type ALK2. Because ATP concentrations within cells vary from 1−10 mM,[42] far in excess of the calculated K_m values, these slight differences in K_m would likely be inconsequential in cells.

A related, long-standing, and clinically relevant question in the FOP field has been whether mutant ALK2 proteins might exhibit differential inhibition by, or distinct affinity for, particular kinase inhibitors, and if so, whether highly specific inhibitors could be engineered to target selectively the activity of these activated mutant proteins. We sought to answer this question by probing a panel of seven representative mutant ALK2 proteins with the library of **K02288** derivatives displaying varying potency against wild-type ALK2 using a thermal shift kinase assay. We found a highly linear correlation (r^2 = 0.94−0.99) between the thermal shift induced by these derivatives with wild-type vs mutant ALK2 proteins (Figure 8).

dx.doi.org/10.1021/jm501177w | J. Med. Chem. 2014, 57, 7900−7915

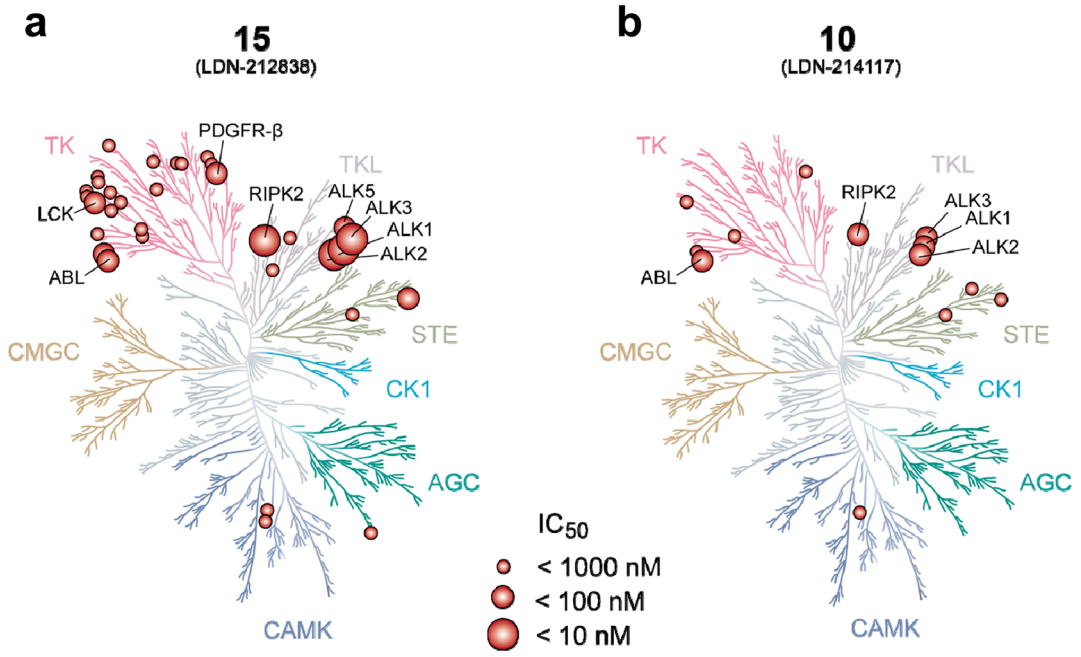

Figure 7. Compound **10** exhibits increased kinome selectivity. Kinome dendrogram plot for compound **15** (LDN-212838) (a) and compound **10** (LDN-214117) (b) showing an improved selectivity profile for **10** for BMP type I receptor kinases.

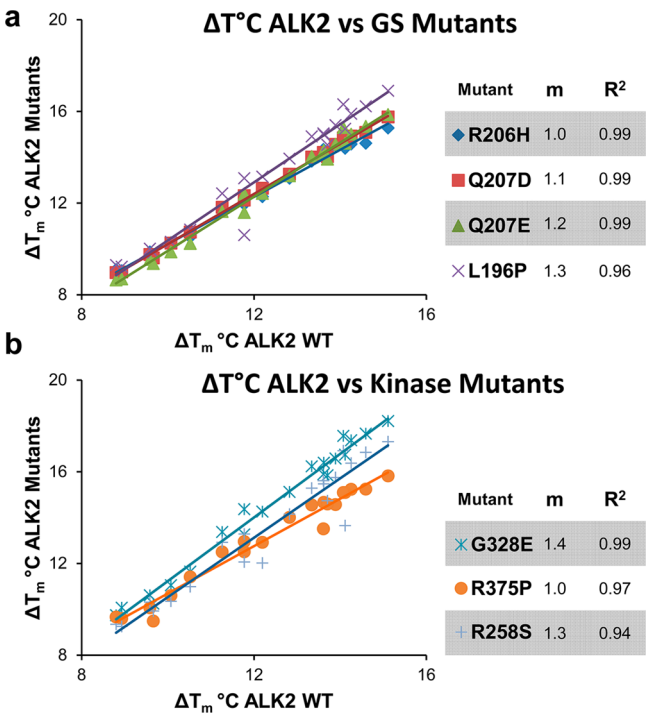

Figure 8. FOP-causing ALK2 mutations do not affect inhibitor binding. (a) Strong correlation of thermal shift data for ATP competitive kinase inhibitors binding to wild-type ALK2 versus known FOP causing GS-domain mutations of ALK2 and (b) known FOP causing kinase domain mutations suggests the potency of ATP competitive inhibitors are not affected by these disease causing mutations. m = slope, R^2 = correlation coefficient.

These results suggest that inhibitors engineered or identified against wild-type or mutant ALK2 proteins will have interchangeable activity against diverse mutant proteins found in FOP or DIPG. Conversely, these results would preclude the development of ATP-competitive ALK2 inhibitors which selectively target mutant proteins. The pathogenicity of activating mutations of ACVR1 has been well-established for FOP, and thus the development of highly selective inhibitors is an important step in validating ALK2 as a feasible clinical target. While the presence of ACVR1 mutations appears to be associated with increased downstream BMP signaling and transcriptional activity in DIPG tumors,[16,18] further work will need to be performed to determine whether or not these mutations contribute to the initiation or progression of tumors in DIPG. The identification of selective inhibitors of ALK2 may help to elucidate the mechanisms of DIPG tumorigenicity and could potentially be therapeutic if a contribution of BMP signaling is confirmed.

Cytotoxicity of Kinase Inhibitors. We next sought to determine the cytotoxicity of these derivatives and to compare them to many of the current FDA approved kinase inhibitors (Figure 9). Because hepatotoxicity is one of the most common reasons for withdrawal of approved drugs, we used HEPG2 cells for evaluation of cytotoxicity.[43] Compounds were tested in a large concentration range (1−100 μM) for 4 and 24 h. Upon the basis of residual cell viability after treatment, compounds were categorized as having low (>75%), medium (25−75%), or high (<25%) cytotoxicity. Of the 12 approved kinase inhibitors tested, only one exhibited high cytotoxicity at 100 μM after 4 h of incubation, whereas six of the 28 derivatives in our **K02288** library exhibited high cytotoxicity after 4 h. Over a 24 h period four of 12 approved kinase inhibitors showed high cytotoxicity at 100 μM, whereas 23 of the 28 **K02288** derivatives showed high toxicity. However, **10**, which demonstrated good potency and high BMP selectivity, exhibited very low cytotoxicity. In fact, cytotoxicity was not correlated with BMP signaling inhibition, TGF-β inhibition, nor selectivity for BMP versus TGF-β signaling (Supporting Information, Figure 5). For example, the highly potent BMP inhibitor **11** was also noncytotoxic, suggesting that the mechanisms of cytotoxicity within this series of compounds do not result from effects on BMP or TGF-β signaling.

dx.doi.org/10.1021/jm501177w | J. Med. Chem. 2014, 57, 7900−7915

Name	4 hr			24 hr		
	1 μM	10 μM	100 μM	1 μM	10 μM	100 μM
Imatinib					72%	13%
Gefitinib						
Sorafenib						7%
Erlotinib						
Dasatinib			75%		75%	38%
Sunitinib			28%		68%	5%
Nilotinib						
Lapatinib						
Pazopanib						
Ruxolitinib						55%
Crizotinib			8%			5%
Vemurafenib						72%
LDN-193189			20%		44%	5%
LDN-212854						6%
K02288						35%
11						
12						
13						
14						10%
15						23%
16						25%
17			68%			5%
18						9%
19						6%
20			17%			5%
21			64%			5%
22			21%			5%
23			35%			5%
24						9%
25						22%
26			62%			5%
27						19%
10						
28			5%			5%
29						24%
30			11%			5%
31						16%
32			65%		65%	5%
33			23%			5%

Figure 9. Cytotoxicity of FDA-approved kinase inhibitor compounds as compared with BMP inhibitor compounds. Cultured HepG2 cells were exposed to 1, 10, and 100 μM concentrations of compounds for 4 and 24 h. The average cell viability of three experiments is shown (green indicating >75%, orange indicating 25−75%, and red <25% viability).

Structural Basis of Inhibitor Binding. A number of the most promising derivatives were tested for co-crystallization with ALK2 to further understand the binding mode and SAR. Diffraction quality crystals were obtained in the presence of **26**, and the structure of the complex was solved at 2.6 Å resolution (Figure 9; see Supporting Information, Table 5 for data collection and refinement statistics).

In the co-crystal structure, **26** was bound to the kinase hinge region as shown previously for the parent molecule **K02288** (Figure 10).[23] Both molecules established an ATP-mimetic hydrogen bond between the pyridine nitrogen and the amide of H286. Replacement of the 3-phenol and primary amine with 4-phenylpiperazine and hydrogen, respectively, did not alter the overall position of **26** but resulted in the loss of the hinge hydrogen bond interaction between the primary amine and the carbonyl of H284. The conserved 3,4,5-trimethoxyphenyl provided hydrophobic interaction as well as a water-mediated hydrogen bond to the catalytic lysine K235. Docking of **10** produced a similar binding mode, with no significant change resulting from the introduction of the methyl group. Overall, the ATP pocket occupied by these 3,5-diarylpyridines was similar to the pyrazolo[1,5-*a*]pyrimidine scaffold of LDN-193189. However, the two series differed slightly in their hinge binding orientation resulting in shifts in the position of their respective hydrophobic pocket groups as well as the shared 4-phenylpiperazine (Supporting Information, Figure 6).

The selectivity of these molecules for ALK2 over ALK5 likely results from dynamic conformational differences between these kinases as well as the modest number of sequence changes in the ATP pocket. Perhaps as a result of its smaller serine gatekeeper residue, the ATP pocket in many ALK5 co-crystal structures shows a more open conformation than those of ALK2 with a noticeable movement of the N-lobe away from the C-lobe (Supporting Information, Figure 1). Such conformational differences are expected to change the shape, volume, and dynamics of the ATP pocket to impact inhibitor binding.

CONCLUSION

We have developed a library of BMP receptor kinase inhibitors based on the 2-aminopyridine scaffold of **K02288**. This library allowed us to explore the SAR of various functional groups and resulted in the creation of several potent derivatives. Several of these compounds demonstrated improved activity, selectivity, or both, measured using a thermal shift assay, an enzymatic assay, and cellular assays of BMP/TGF-β-induced transcription,

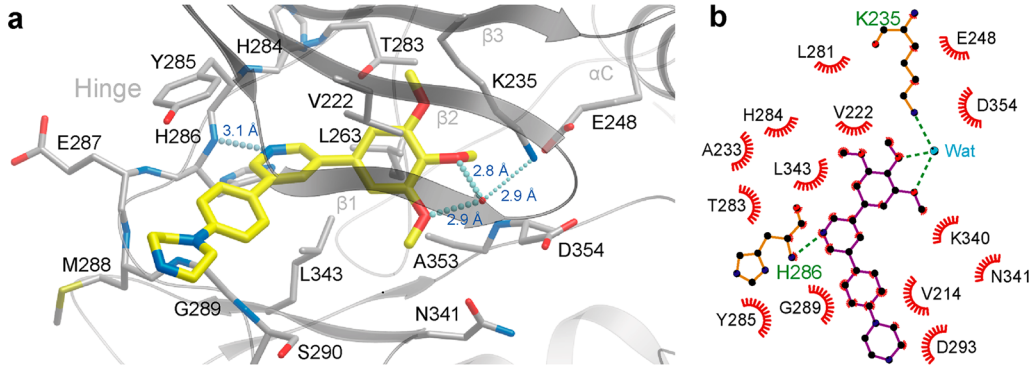

Figure 10. Binding mode of **26**. (a) The inhibitor (yellow) forms a single hydrogen bond to the hinge amide of H286 as well as a water-mediated bond to the catalytic lysine K235. (b) Plot of the interactions of the inhibitor (purple) in the binding pocket of ALK2. The plot was generated by LigPlot+.[54]

dx.doi.org/10.1021/jm501177w | J. Med. Chem. 2014, 57, 7900−7915

thus overcoming the limited potency of the parent compound in cells.

We determined that the solvent-exposed 3-phenol substituent of **K02288** was responsible for its unexpectedly low activity in cells as compared to kinase assay IC_{50}. By replacing this group with either a 4-phenol or 4-phenylpiperazine, we were able to improve potency in cellular assays compared to **K02288** by 20- and 100-fold, respectively. We previously reported that the 3,4,5-trimethoxyphenyl occupies the rear hydrophobic pocket to provide excellent shape complementarity and forms water-mediated hydrogen bonds to the catalytic lysine residue (K235).[23] Here we found that the 4-methoxy group was largely dispensable, while the 3- or 5-methoxy groups were more critical for maintaining potency. The balance of selectivity and potency found in the 3,5-dimethoxy derivative **17** suggests further medicinal chemistry optimization is possible and could yield further insights into the determinants of activity in the hydrophobic pocket. Within the 2-aminopyridine core, we found that the primary amine was more critical for TGF-β than BMP binding affinity and could be replaced with a nonpolar methyl group to generate a highly BMP selective compound **10** (LDN-214117), which is significantly biased toward ALK2 and its cognate ligands including BMP6 and also demonstrates a high degree of kinome selectivity and low cytotoxicity. Finally, we concluded that replacing the 3,4,5-trimethoxyphenyl with quinolines as previously described for pyrazolopyrimidine compounds (LDN-193189 and LDN-212854) was not an effective strategy and resulted in a substantial loss of potency.

We used this structurally diverse compound series with varying degrees of potency to explore the effect of FOP-causing mutations on inhibitor binding affinity. These compounds exhibited nearly identical binding affinity for wild-type ALK2 and each of the FOP-causing mutants tested, demonstrating that ATP-competitive inhibitors active against wild-type protein will effectively target diverse FOP mutants. While this result would also suggest that ATP-competitive inhibitors cannot specifically target mutant versus wild-type ALK2, one could envision molecules targeting allosteric sites unique to mutant proteins to potentially achieve specificity.

The novel series of compounds reported here constitutes an alternative pharmacophore with discrete properties, including distinct kinome selectivity, as compared to the pyrazolopyrimidine class of BMP inhibitors.[23] Several of these compounds, including **10** (LDN-214117), may be useful as highly selective probes of BMP-mediated cellular physiology that may provide a useful complement to the dorsomorphin class of compounds. Furthermore, this class of BMP inhibitors offers a structurally distinct template for the development of therapeutics for the treatment of BMP signaling-mediated diseases such as FOP.

EXPERIMENTAL SECTION

Chemistry Material and Methods. Unless otherwise noted, all reagents and solvents were purchased from commercial sources and used without further purification. The NMR spectra were obtained using a 300 or 500 MHz spectrometer. All ^{1}H NMR spectra are reported in δ units (ppm) and were recorded in $CDCl_3$ and referenced to the peak for tetramethylsilane (TMS) or in DMSO. Coupling constants (J) are reported in hertz. Column chromatography was performed utilizing a CombiFlash Sg 100c separation system with RediSep disposable silica gel columns. High-resolution mass spectra were obtained by using AccuTOF with a DART source. All test compounds reported in this manuscript had a purity ≥95% as determined by high-performance liquid chromatography (HPLC) analyses using an instrument equipped with a quaternary pump and a SB-C8 column (30 mm × 4.6 mm, 3.5 μm). UV absorption was monitored at λ = 254 nm. The injection volume was 5 μL. HPLC gradient went from 5% acetonitrile/95% water to 95% acetonitrile/5% water (both solvents contain 0.1% trifluoroacetic acid) over 1.9 min with a total run time of 3.0 min and a flow rate of 3.0 mL/min.

Synthesis of 2-Amino-5-bromo-3-(3,4,5-trimethoxyphenyl)-pyridine (2). A mixture of 5-bromo-3-iodopyridin-2-amine (386 mg, 1.30 mmol), 3,4,5-trimethoxyphenylboronic acid (275 mg, 1.30 mmol), and $Pd(PPh_3)_4$ (180 mg, 0.156 mmol) were added to a sealed tube. The tube was evacuated and backfilled with argon (3 cycles). Acetonitrile (6.0 mL) and DMF (2.5 mL) were added by syringe at room temperature, followed by (1 M) aqueous Na_2CO_3 (2.6 mL, 2.60 mmol). After being stirred at 90 °C for about 8 h, the reaction mixture was filtered and concentrated. The residue was purified by flash column chromatography to give **2** as white solid (235 mg, 80%). ^{1}H NMR (500 MHz, $CDCl_3$) δ 8.11 (d, J = 2.5 Hz, 1H), 7.48 (d, J = 2.5 Hz, 1H), 6.62 (s, 2H), 3.90 (s, 3H), 3.88 (s, 6H). MS (ESI): 339.0 $[M]^+$.

General Synthesis of 2-Amino-5-aryl-3-(3,4,5-trimethoxyphenyl)pyridines (3). To a solution of **2** (1.0 equiv), an aryl boronic acid (1.1 equiv), and $Pd(PPh_3)_4$ (0.12 equiv) in DME, (1 M) aqueous Na_2CO_3 (2.0 equiv) was added. The reaction mixture was stirred under an argon atmosphere at 90 °C for 8 h. The reaction mixture was filtered and then concentrated. The residue was purified by flash column chromatography, eluting with a mixture of cyclohexane and EtOAc to give products **3**.

3-(6-Amino-5-(3,4,5-trimethoxyphenyl)pyridin-3-yl)phenol (K02288). Yield: 40%. ^{1}H NMR (500 MHz, $CDCl_3$) δ 8.48 (d, J = 2.0 Hz, 1H), 7.69 (d, J = 2.0 Hz, 1H), 7.34 (t, J = 7.5 Hz, 1H), 7.20 (d, J = 2.0 Hz, 1H), 7.08 (d, J = 8.0 Hz, 1H), 6.90 (dd, J = 2.0, 7.0 Hz, 1H), 6.68 (s, 2H), 4.81 (br, 2H), 3.91 (s, 3H), 3.89 (s, 6H). HRMS (ESI) calcd for $C_{20}H_{21}N_2O_4$ 353.1501 $[M + H]^+$; found 353.1462; purity 95.6% (t_R 1.35 min).

4-(6-Amino-5-(3,4,5-trimethoxyphenyl)pyridin-3-yl)phenol (11). Yield: 42%. ^{1}H NMR (500 MHz, $CDCl_3$) δ 8.27 (d, J = 2.5 Hz, 1H), 7.57 (d, J = 2.5 Hz, 1H), 7.43−7.41 (m, 2H), 6.92−6.90 (m, 2H), 6.90 (dd, J = 2.0, 7.0 Hz, 1H), 6.69 (s, 2H), 4.64 (br, 2H), 3.91 (s, 3H), 3.89 (s, 6H). HRMS (ESI) calcd for $C_{20}H_{21}N_2O_4$ 353.1501 $[M + H]^+$; found 353.1490; purity 100.0% (t_R 1.32 min).

4-(6-Amino-5-(3,4,5-trimethoxyphenyl)pyridin-3-yl)-2-methoxyphenol (12). Yield: 70%. ^{1}H NMR (500 MHz, $CDCl_3$) δ 8.27 (d, J = 2.5 Hz, 1H), 7.56 (d, J = 2.5 Hz, 1H), 7.06−6.98 (m, 3H), 6.70 (s, 2H), 4.65 (br, 2H), 3.95 (s, 3H), 3.91 (s, 3H), 3.89 (s, 6H). HRMS (ESI) calcd for $C_{21}H_{23}N_2O_5$ 383.1607 $[M + H]^+$; found 383.1603; purity 98.3% (t_R 1.34 min).

***N*-(3-(6-Amino-5-(3,4,5-trimethoxyphenyl)pyridin-3-yl)-phenyl)methanesulfonamide (13).** Yield: 85%. ^{1}H NMR (500 MHz, $CDCl_3$) δ 8.89 (br, 1H), 8.39 (d, J = 2.5 Hz, 1H), 7.61 (d, J = 1.5 Hz, 1H), 7.47−7.40 (m, 3H), 7.34 (dt, J = 1.5, 7.5 Hz, 1H), 6.68 (s, 2H), 5.19 (br, 2H), 3.91 (s, 3H), 3.90 (s, 6H) 3.06 (s, 3H). HRMS (ESI) calcd for $C_{21}H_{24}N_3O_5S$ 430.1437 $[M + H]^+$; found 430.1412; purity 99.3% (t_R 1.34 min).

General Synthesis of 3-Aryl-5-bromopyridines (5). A mixture of 5-bromo-3-iodopyridin-2-amine (1.0 equiv), arylboronic acid (1.0 equiv), and $Pd(PPh_3)_4$ (0.12 equiv) was added to a sealed tube. The tube was evacuated and backfilled with argon (3 cycles). Acetonitrile and DMF (3:1 mL) were added by syringe at room temperature, followed by (1 M) aqueous Na_2CO_3 (2.0 equiv). After being stirred at 90 °C for about 8 h, the reaction mixture was filtered and concentrated. The residue was purified by flash column chromatography to give **5**.

General Synthesis of 3-Aryl-5-((*N*-Boc)-piperazinylphenyl)-pyridines (6). To a solution of **5** (1.0 equiv), [(*N*-Boc)piperazin-1-yl]phenylboronic acid pinacol ester (1.1 equiv), and $Pd(PPh_3)_4$ (0.12 equiv) in DME, (1 M) aqueous Na_2CO_3 (2.0 equiv) was added. The reaction mixture was stirred under argon atmosphere at 90 °C for 8 h. The reaction mixture was filtered and concentrated. The residue was purified by flash column chromatography, eluting with a mixture cyclohexane/EtOAc to give **6**.

dx.doi.org/10.1021/jm501177w | J. Med. Chem. 2014, 57, 7900−7915

General Synthesis of 3-Aryl-5-(piperazinylphenyl)pyridines (7). To a stirring solution of the **6** (0.01 mmol) in dry CH_2Cl_2 (2 mL) at 0 °C, trifluoroacetic acid (0.2 mL) was slowly added and the reaction mixture was stirred overnight at room temperature. The mixture was concentrated under vacuum. The residue was suspected in ethyl acetate (10 mL), and then a saturated $NaHCO_3$ solution was added to adjust the pH to 7 at 0 °C. The mixture was extracted with ethyl acetate (3 × 10 mL). The combined organic layer was dried over anhydrous Na_2SO_4, filtered, and concentrated in vacuo. The remaining residue was subjected to column chromatography to furnish 7 as a white to light-yellow foam.

5-(3-(Piperazin-1-yl)phenyl)-3-(3,4,5-trimethoxyphenyl)-pyridin-2-amine (14). Yield: 82%. ^{1}H NMR (500 MHz, $CDCl_3$) δ 8.31 (d, J = 2.5 Hz, 1H), 7.61 (d, J = 2.5 Hz, 1H), 7.35 (d, J = 8.0 Hz, 1H), 7.07 (t, J = 2.0 Hz, 1H), 7.04−7.03 (m, 1H), 6.92−6.90 (m, 1H), 6.70 (s, 2H), 4.68 (br, 2H), 3.91 (s, 3H), 3.89 (s, 6H), 3.21−3.19 (m, 4H), 3.06−3.04 (m, 4H). HRMS (ESI) calcd for $C_{24}H_{28}N_4O_3$ 421.2240 $[M + H]^+$; found 421.2215; purity 98.7% (t_R 1.12 min).

5-(4-(Piperazin-1-yl)phenyl)-3-(3,4,5-trimethoxyphenyl)-pyridin-2-amine (15). Yield: 77%. ^{1}H NMR (500 MHz, $CDCl_3$) δ 8.29 (d, J = 2.0 Hz, 1H), 7.58 (d, J = 2.5 Hz, 1H), 7.47−7.45 (m, 2H), 7.00−6.98 (m, 2H), 6.70 (s, 2H), 4.61 (br, 2H), 3.91 (s, 3H), 3.89 (s, 6H), 3.26−3.24 (m, 0.6H) and 3.20−3.18 (m, 3.4H) due to rotamer, 3.07−3.05 (m, 3.4H) and 2.72−2.70 (m, 0.6H) due to rotamer. HRMS (ESI) calcd for $C_{24}H_{28}N_4O_3$ 421.2240 $[M + H]^+$; found 421.2259; purity 98.6% (t_R 1.05 min).

3-(3,4-Dimethoxyphenyl)-5-(4-(piperazin-1-yl)phenyl)-pyridin-2-amine (16). Yield: 80%. ^{1}H NMR (500 MHz, $CDCl_3$) δ 8.28 (d, J = 2.5 Hz, 1H), 7.57 (d, J = 2.0 Hz, 1H), 7.47−7.45 (m, 2H), 7.06−7.04 (m, 1H), 7.01−6.97 (m, 4H), 4.58 (br, 2 H), 3.94 (s, 3 H), 3.91 (s, 3 H), 3.26−3.24 (m, 0.3H) and 3.20−3.18 (m, 3.7H) due to rotamer, 3.07−3.05 (m, 3.7H) and 2.72−2.70 (m, 0.3H) due to rotamer. HRMS (ESI) calcd for $C_{23}H_{27}N_4O_2$ 391.2134 $[M + H]^+$; found 391.2142; purity 97.9% (t_R 1.08 min).

3-(3,5-Dimethoxyphenyl)-5-(4-(piperazin-1-yl)phenyl)-pyridin-2-amine (17). Yield: 85%. ^{1}H NMR (500 MHz, $CDCl_3$) δ 8.27 (d, J = 2.5 Hz, 1H), 7.59 (d, J = 2.5 Hz, 1H), 7.46−7.44 (m, 2H), 7.00−6.98 (m, 2H), 6.63 (d, J = 2.0 Hz, 2H), 6.50 (t, J = 2.5 Hz, 1H), 4.76 (br, 2H), 3.83 (s, 6H), 3.21−3.19 (m, 4H), 3.08−3.06 (m, 4H). HRMS (ESI) calcd for $C_{23}H_{27}N_4O_2$ 391.2134 $[M + H]^+$; found 391.2159; purity 97.7% (t_R 1.16 min).

3-(3-Methoxyphenyl)-5-(4-(piperazin-1-yl)phenyl)pyridin-2-amine (18). Yield: 82%. ^{1}H NMR (500 MHz, $CDCl_3$) δ 8.28 (d, J = 2.0 Hz, 1H), 7.59 (d, J = 2.0 Hz, 1H), 7.46−7.44 (m, 2H), 7.41 (t, J = 8.0 Hz, 1H), 7.09−7.07 (m, 1H), 7.03 (t, J = 2.0 Hz, 1H), 7.00−6.98 (m, 2H), 6.95 (dd, J = 2.0, 8.5 Hz, 1H), 4.69 (br, 2 H), 3.85 (s, 3H), 3.26−3.24 (m, 0.7H) and 3.22−3.20 (m, 3.3H) due to rotamer, 3.09−3.07 (m, 3.3H) and 2.72−2.70 (m, 0.7H) due to rotamer. HRMS (ESI) calcd for $C_{22}H_{25}N_4O$ 361.2028 $[M + H]^+$; found 361.2043; purity 97.5% (t_R 1.16 min).

3-(2,3-Dihydrobenzo[*b*][1,4]dioxin-6-yl)-5-(4-(piperazin-1-yl)phenyl)pyridin-2-amine (19). Yield: 80%. ^{1}H NMR (500 MHz, $CDCl_3$) δ 8.25 (d, J = 2.5 Hz, 1H), 7.54 (d, J = 2.0 Hz, 1H), 7.45−7.43 (m, 2H), 7.02−7.01 (m, 1H), 6.99−6.96 (m, 4H), 4.63 (br, 2H), 4.31 (s, 4 H), 3.25−3.23 (m, 0.8H) and 3.20−3.18 (m, 3.2H) due to rotamer, 3.07−3.05 (m, 3.2H) and 2.72−2.70 (m, 0.8H) due to rotamer. HRMS (ESI) calcd for $C_{23}H_{25}N_4O_2$ 389.1978 $[M + H]^+$; found 389.2003; purity 97.0% (t_R 1.16 min).

3-(4-Methoxyphenyl)-5-(4-(piperazin-1-yl)phenyl)pyridin-2-amine (20). Yield: 78%. ^{1}H NMR (500 MHz, $CDCl_3$) δ 8.27 (d, J = 2.5 Hz, 1H), 7.55 (d, J = 2.0 Hz, 1H), 7.46−7.42 (m, 4H), 7.02−6.98 (m, 4H), 4.55 (br, 2H), 3.87 (s, 3H), 3.19−3.18 (m, 4H), 3.07−3.05 (m, 4H). HRMS (ESI) calcd for $C_{22}H_{25}N_4O$ 361.2028 $[M + H]^+$; found 361.2055; purity 97.7% (t_R 1.20 min).

3-(3-Isopropoxyphenyl)-5-(4-(piperazin-1-yl)phenyl)pyridin-2-amine (21). Yield: 80%. ^{1}H NMR (300 MHz, $CDCl_3$) δ 8.29 (d, J = 2.4 Hz, 1H), 7.58 (d, J = 2.4 Hz, 1H), 7.47−7.44 (m, 2H), 7.39 (d, J = 8.4 Hz, 1H), 7.06−6.97 (m, 4H), 6.93−6.89 (m, 1H), 4.63−4.55 (m, 3H), 3.20−3.17 (m, 4H), 3.07−3.04 (m, 4H), 1.37 (d, J = 6.0 Hz, 6H). HRMS (ESI) calcd for $C_{24}H_{29}N_4O$ 389.2341 $[M + H]^+$; found 389.2362; purity 100.0% (t_R 1.16 min).

3-(4-Chloro-3-methoxyphenyl)-5-(4-(piperazin-1-yl)phenyl)-pyridin-2-amine (22). Yield: 82%. ^{1}H NMR (300 MHz, $CDCl_3$) δ 8.27 (d, J = 2.1 Hz, 1H), 7.57 (d, J = 2.4 Hz, 1H), 7.48−7.44 (m, 3H), 7.04−6.98 (m, 4H), 4.83 (br, 2H), 3.94 (s, 3H), 3.32−3.29 (m, 3.6H) and 3.26−3.22 (m, 0.4H) due to rotamer, 3.18−3.15 (m, 3.6H) and 2.74−2.69 (m, 0.4H) due to rotamer. HRMS (ESI) calcd for $C_{22}H_{24}ClN_4O$ 395.1639 $[M + H]^+$; found 395.1647; purity 96.6% (t_R 1.18 min).

3-(3-Methoxy-4-methylphenyl)-5-(4-(piperazin-1-yl)phenyl)-pyridin-2-amine (23). Yield: 84%. ^{1}H NMR (300 MHz, $CDCl_3$) δ 8.28 (d, J = 2.4 Hz, 1H), 7.58 (d, J = 2.4 Hz, 1H), 7.47−7.44 (m, 2H), 7.24−7.21 (m, 1H), 7.00−6.97 (m, 3H), 6.93 (d, J = 1.5 Hz, 1H), 4.65 (br, 2H), 3.85 (s, 3H), 3.20−3.16 (m, 4H), 3.07−3.03 (m, 4H), 2.67 (s, 3H). HRMS (ESI) calcd for $C_{23}H_{27}N_4O$ 375.2185 $[M + H]^+$; found 375.2189; purity 100.0% (t_R 1.16 min).

***N*-Methyl-5-(4-(piperazin-1-yl)phenyl)-3-(3,4,5-trimethoxyphenyl)pyridin-2-amine (24).** Yield: 92%. ^{1}H NMR (500 MHz, $CDCl_3$) δ 8.39 (d, J = 2.0 Hz, 1H), 7.50 (d, J = 2.5 Hz, 1H), 7.46−7.45 (m, 2H), 7.00−6.98 (m, 2H), 6.63 (s, 2H), 4.67 (q, J = 5.0 Hz, 1H), 3.91 (s, 3H), 3.88 (s, 6H), 3.25−3.22 (m, 0.6H) and 3.20−3.18 (m, 3.4H) due to rotamer, 3.08−3.06 (m, 3.6H) and 2.72−2.70 (m, 0.4H) due to rotamer, 3.01 (d, J = 5.0 Hz, 3H). HRMS (ESI) calcd for $C_{25}H_{31}N_4O_3$ 435.2396 $[M + H]^+$; found 435.2396; purity 98.9% (t_R 1.10 min).

***N*,*N*-Dimethyl-5-(4-(piperazin-1-yl)phenyl)-3-(3,4,5-trimethoxyphenyl)pyridin-2-amine (25).** Yield: 90%. ^{1}H NMR (500 MHz, $CDCl_3$) δ 8.40 (d, J = 2.0 Hz, 1H), 7.62 (d, J = 2.5 Hz, 1H), 7.48−7.46 (m, 2H), 7.00−6.99 (m, 2H), 6.76 (s, 2H), 3.90 (s, 3H), 3.88 (s, 6H), 3.21−3.19 (m, 4H), 3.07−3.05 (m, 4H), 2.78 (s, 6H). HRMS (ESI) calcd for $C_{26}H_{33}N_4O_3$ 449.2553 $[M + H]^+$; found 449.2575; purity 97.8% (t_R 1.14 min).

1-(4-(5-(3,4,5-Trimethoxyphenyl)pyridin-3-yl)phenyl)-piperazine (26). Yield: 95%. ^{1}H NMR (500 MHz, $CDCl_3$) δ 8.78 (d, J = 2.0 Hz, 1H), 8.71 (d, J = 2.5 Hz, 1H), 7.95 (t, J = 2.5 Hz, 1H), 7.58−7.56 (m, 2H), 7.06−7.04 (m, 2H), 6.80 (s, 2H), 3.95 (s, 6H), 3.91 (s, 3H), 3.25−3.23 (m, 4H), 3.08−3.06 (m, 4H). HRMS (ESI) calcd for $C_{24}H_{28}N_3O_3$ 406.2131 $[M + H]^+$; found 406.2142; purity 100.0% (t_R 1.20 min).

1-(4-(6-Chloro-5-(3,4,5-trimethoxyphenyl)pyridin-3-yl)-phenyl)piperazine (27). Yield: 94%. ^{1}H NMR (300 MHz, $CDCl_3$) δ 8.57 (d, J = 2.4 Hz, 1H), 7.83 (d, J = 2.7 Hz, 1H), 7.53−7.50 (m, 2H), 7.03−7.00 (m, 2H), 6.70 (s, 2H), 3.92 (s, 3H), 3.90 (s, 6H), 3.32−3.28 (m, 0.5H) and 3.27−3.24 (m, 3.5H) due to rotamer, 3.10−3.07 (m, 3.5H) and 2.75−2.69 (m, 0.5H) due to rotamer. HRMS (ESI) calcd for $C_{24}H_{27}ClN_3O_3$ 440.1741 $[M + H]^+$; found 440.1723; purity 95.6% (t_R 1.42 min).

1-(4-(6-Methoxy-5-(3,4,5-trimethoxyphenyl)pyridin-3-yl)-phenyl)piperazine (28). Yield: 79%. ^{1}H NMR (500 MHz, $CDCl_3$) δ 8.34 (d, J = 2.0 Hz, 1H), 7.78 (d, J = 2.5 Hz, 1H), 7.50−7.48 (m, 2H), 7.03−7.01 (m, 2H), 6.81 (s, 2H), 4.02 (s, 3H), 3.90 (s, 9H), 3.28−3.26 (m, 0.3H) and 3.23−3.21 (m, 3.7H) due to rotamer, 3.08−3.07 (m, 3.7H) and 2.73−2.71 (m, 0.3H) due to rotamer. HRMS (ESI) calcd for $C_{25}H_{29}N_3O_4$ 436.2236 $[M + H]^+$; found 436.2265; purity 100.0% (t_R 1.38 min).

5-(4-(Piperazin-1-yl)phenyl)-3-(quinolin-4-yl)pyridin-2-amine (29). Yield: 79%. ^{1}H NMR (500 MHz, $CDCl_3$) δ 9.02 (d, J = 4.5 Hz, 1H), 8.46 (d, J = 2.5 Hz, 1H), 8.22 (d, J = 8.0 Hz, 1H), 7.79−7.75 (m, 2H), 7.64 (d, J = 2.5 Hz, 1H), 7.57−7.53 (m, 1H), 7.48−7.43 (m, 3H), 7.01−6.98 (m, 2H), 4.34 (br, 2H), 3.25−3.23 (m, 0.6H) and 3.20−3.18 (m, 3.4H) due to rotamer, 3.07−3.05 (m, 3.4H) and 2.72−2.70 (m, 0.6H) due to rotamer. HRMS (ESI) calcd for $C_{24}H_{24}N_5$ 382.2032 $[M + H]^+$; found 382.1993; purity 97.7% (t_R 1.04 min).

5-(3-(Piperazin-1-yl)phenyl)-3-(quinolin-4-yl)pyridin-2-amine (30). Yield: 85%. ^{1}H NMR (500 MHz, $CDCl_3$) δ 9.03 (d, J = 4.0 Hz, 1H), 8.48 (s, 1 H), 8.22 (d, J = 8.0 Hz, 1H), 7.80−7.74 (m, 2H), 7.66 (s, 1 H), 7.57 (d, J = 8.0 Hz, 1H), 7.47−7.44 (m, 1H), 7.35 (t, J = 8.0 Hz, 1H), 7.07−7.03 (m, 2H), 6.92 (d, J = 8.5 Hz, 1H), 4.38 (br, 2 H), 3.26−3.22 (m, 1H) and 3.21−3.19 (m, 3H) due to rotamer, 3.05−3.04 (m, 3H) and 2.71−2.66 (m, 1H) due to rotamer. HRMS (ESI) calcd for $C_{24}H_{24}N_5$ 382.2032 $[M + H]^+$; found 382.2024; purity 95.1% (t_R 1.09 min).

dx.doi.org/10.1021/jm501177w | *J. Med. Chem.* 2014, 57, 7900−7915

5-(4-(Piperazin-1-yl)phenyl)-3-(quinolin-5-yl)pyridin-2-amine (31). Yield: 84%. ^{1}H NMR (500 MHz, $CDCl_3$) δ 8.98 (dd, J = 2.0, 4.5 Hz, 1H), 8.44 (d, J = 2.5 Hz, 1H), 8.21 (d, J = 9.0 Hz, 1H), 8.06−8.04 (m, 1H), 7.84−7.81 (m, 1H), 7.63 (d, J = 2.5 Hz, 1H), 7.59−7.58 (m, 1H), 7.48−7.46 (m, 2H), 7.41−7.39 (m, 1H), 7.00−6.97 (m, 2H), 4.29 (br, 2 H), 3.25−3.23 (m, 0.4H) and 3.20−3.18 (m, 3.6H) due to rotamer, 3.06−3.04 (m, 3.6H) and 2.71−2.69 (m, 0.4H) due to rotamer. HRMS (ESI) calcd for $C_{24}H_{24}N_5$ 382.2032 $[M + H]^+$; found 382.2039; purity 95.2% (t_R 0.97 min).

1-(4-(5-(3,5-Dimethoxyphenyl)pyridin-3-yl)phenyl)-piperazine (33). Yield: 98%. ^{1}H NMR (300 MHz, $CDCl_3$) δ 8.79 (d, J = 2.4 Hz, 1H), 8.73 (d, J = 2.4 Hz, 1H), 7.99 (t, J = 2.1 Hz, 1H), 7.57−7.54 (m, 2H), 7.04−7.02 (m, 2H), 6.76 (d, J = 1.8 Hz, 2H), 6.53 (t, J = 2.1 Hz, 1H), 3.86 (s, 6H), 3.23−3.21 (m, 4H), 3.06−3.04 (m, 4H). HRMS (ESI) calcd for $C_{23}H_{26}N_3O_2$ 376.2025 $[M + H]^+$; found 376.2023; purity 100.0% (t_R 1.26 min).

Synthesis of 1-(4-(6-Methyl-5-(3,4,5-trimethoxyphenyl)-pyridin-3-yl)phenyl)piperazine (10). A mixture of *N*-Boc-4-(4-(6-chloro-5-(3,4,5-trimethoxyphenyl)pyridin-3-yl)phenyl)piperazine (43 mg, 0.080 mmol), trimethylboroxine (46 μL, 0.32 mmol), $Pd(PPh_3)_4$ (19 mg, 0.016 mmol), and K_2CO_3 (22 mg, 0.16 mmol) were added to a sealed tube. The tube was evacuated and backfilled with argon (3 cycles). 1,4-Dioxane (1.0 mL) was added by syringe at room temperature. After being stirred at 110 °C for 8 h, the reaction mixture was filtered and concentrated. The residue purified by flash column chromatography to give **9** (40 mg, 96%). ^{1}H NMR (300 MHz, $CDCl_3$) δ 8.70 (d, J = 2.4 Hz, 1H), 7.69 (d, J = 2.4 Hz, 1H), 7.54−7.51 (m, 2H), 7.02−6.99 (m, 2H), 6.55 (s, 2H), 3.91 (s, 3H), 3.88 (s, 6H), 3.61−3.58 (m, 4H), 3.21−3.18 (m, 4H), 2.55 (s, 3H), 1.48 (s, 9H). MS (ESI): 519.5 $[M]^+$. The carbamate protecting group of **9** (40 mg) was removed using the general method previously described using TFA to furnish **10** as a white foam (30 mg, 93%). ^{1}H NMR (300 MHz, $CDCl_3$) δ 8.71 (d, J = 2.1 Hz, 1H), 7.70 (d, J = 2.4 Hz, 1H), 7.55−7.52 (m, 2H), 7.03−7.00 (m, 2H), 6.56 (s, 2H), 3.92 (s, 3H), 3.89 (s, 6H), 3.24−3.20 (m, 4H), 3.08−3.05 (m, 4H), 2.55 (s, 3H). HRMS (ESI) calcd for $C_{25}H_{30}N_3O_3$ 420.2287 $[M + H]^+$; found 420.2295; purity 95.5% (t_R 1.13 min).

Synthesis of 3-(3,4,5-Trimethoxyphenyl)-6-[4-(1-piperazinyl)phenyl]pyrazolo[1,5-*a*]pyrimidine (32). This compound was prepared using a reported methodology.[9] ^{1}H NMR (500 MHz, DMSO) δ 9.38 (d, J = 2.0 Hz, 1H), 9.04 (d, J = 2.0 Hz, 1H), 8.80 (s, 1H), 7.75 (d, J = 9.0 Hz, 2H), 7.51 (s, 2H), 7.07 (d, J = 9.0 Hz, 1H), 3.88 (s, 6H), 3.70 (s, 3H), 3.25−3.18 (m, 4H), 2.92−2.90 (m, 4H). HRMS (ESI) calcd for $C_{25}H_{27}N_5O_3$ 446.2192 $[M + H]$+; found 446.2186; purity 100% (t_R 1.43 min).

Thermal Shift Kinase Assay. Thermal melting experiments were performed using a Real Time PCR machine Mx3005p (Stratagene) with a protein concentration of 1−2 μM and 10 μM inhibitor as described previously.[44] Recombinant human kinases for DSF screening were prepared by SGC using published methods.[23]

Protein Expression and Purification. The human ALK2 kinase domain, residues 201−499 including the activating mutation Q207D, was subcloned into the vector pFB-LIC-Bse. Baculoviral expression was performed in Sf9 insect cells at 27 °C, shaking at 110 rpm. Cells were harvested at 72 h postinfection and resuspended in 50 mM HEPES pH 7.5, 500 mM NaCl, 5 mM imidazole, 5% glycerol, 0.1 mM TCEP, supplemented with protease inhibitor set V (Calbiochem). Cells were lysed using a C5 high pressure homogenizer (Emulsiflex) and the insoluble material excluded by centrifugation at 21000 rpm. Nucleic acids were removed on a DEAE-cellulose column before purification of the N-terminally His-tagged ALK2 protein by Ni-affinity chromatography. The eluted protein was cleaved with TEV protease and further purified by size exclusion chromatography using a S200 HiLoad 16/60 Superdex column. A final clean up step was performed by reverse purification on a Ni-sepharose column and the purified protein stored at −80 °C.

X-ray Crystallography. Protein was concentrated to 10 mg/mL buffered in 50 mM HEPES, pH 7.5, 300 mM NaCl, 10 mM DTT, 50 mM L-arginine, and 50 mM L-glutamate. Crystallization was performed using the sitting drop vapor diffusion method at 4 °C. Viable crystals of ALK2 in complex with **26** grew in a 150 nL drop, mixing the protein, preincubated with 1 mM compound, with a reservoir solution containing 0.2 M ammonium citrate and 20% PEG 3350 at 2:1 volume ratio. Crystals were transferred into a cryoprotective solution prepared from the mother liquor supplemented with 25% ethylene glycol. Diffraction data were collected at Diamond Light Source, beamline I04-I, and were processed and scaled with MOSFLM and AIMLESS from the CCP4 suite.[45] The crystals formed in space group *I*121 and contained four protein molecules in the asymmetric unit. The structure was solved by molecular replacement using PHASER[46] and the structure of the ALK2-LDN-193189 complex (PDB 3Q4U) as a search model. Subsequent manual model building was performed using COOT[47] alternated with refinement in REFMAC.[48] TLS-restrained refinement was applied in the latter cycles using the input thermal motion parameters determined by the TLSMD server.[49] The final model was verified for geometry correctness with PHENIX validation tools and MOLPROBITY.[50,51] Data collection and refinement statistics are summarized in Supporting Information, Table 5.

Kinase Assay. Purified recombinant ALK2 and ALK5 kinase proteins (Invitrogen), ATP (Sigma), ATP [γ-^{32}P] (PerkinElmer), and dephosphorylated casein (Sigma) at final concentrations of 2.5 nM, 6 μM, 0.05 μCi μL^{-1}, and 0.5 mg mL^{-1}, respectively, were aliquoted in kinase buffer (Cell Signaling) containing 0.2% bovine serum albumin supplemented with 10 mM $MnCl_2$ into 96-microwell plates, in combination with inhibitor compounds diluted at varying concentrations in kinase buffer (0.01 nM to 100 μM) in triplicate. In other experiments, purified recombinant ALK2 mutant kinase proteins[34] were incubated with γ-^{32}P and substrate under similar conditions, but in the presence of varying concentrations of unlabeled ATP, for the determination of K_m and V_{max} for each ALK2 mutant. Positive control samples lacking inhibitor compounds, and negative controls lacking recombinant kinase, were also measured in triplicate. The mixture was reacted at RT for 45 min, quenched with a final concentration of 2% phosphoric acid. The reaction mixture was transferred to 96-well P81 phosphocellulose filter plates (Millipore) and bound for 5 min. The plates were washed 20 times with 150 μL of 1% phosphoric acid solution per well by vacuum manifold. Plates were dried at RT for 1 h, sealed, and assayed with Microscint 20 scintillation fluid (PerkinElmer) using a Spectramax L luminometer (Molecular Devices) using the photon counting setting with an integration time of one second per well. Data was normalized to positive controls at 100% enzyme activity, with negative controls being subtracted as background. GraphPad (Prism software) was used for graphing and regression analysis by sigmoidal dose−response with variable Hill coefficient, or by Michaelis−Menten analysis for the determination of K_m.

Luciferase Reporter Assay. C2C12 myofibroblasts cells stably transfected with BMP responsive element from the Id1 promoter fused to luciferase reporter gene (BRE-Luc) were generously provided by Dr. Peter ten Dijke (Leiden University Medical Center, NL).[52] Human embryonic kidney 293T cells stably transfected with the TGF-β responsive element from the PAI-1 promoter fused to luciferase reporter gene (CAGA-Luc) were generously provided by Dr. Howard Weiner (Brigham and Women's Hospital, Boston, MA).[53] C2C12 Bre-Luc and 293T CAGA-Luc cells were seeded in DMEM supplemented with 2% FBS at 20000 cells per well in tissue culture treated 96-well plates (Costar 3610; Corning). The cells were incubated for 1 h (37 °C and 10% CO_2) and allowed to settle and attach. Compounds of interest or DMSO were diluted in DMEM and added at final compound concentrations of 1 nM to 10 μM. Cells were then incubated for 30 min. Adenovirus expressing constitutively active BMP and TGF-β type I receptors (Ad.caALK1−5), generously provided by Dr. Akiko Hata (University of California at San Francisco), were added to achieve a multiplicity of infection (MOI) of 100. Plates were incubated overnight at 37 °C. Cell viability was assayed with an 3-(4,5-dimethylthiazol-2-yl)-2,5-diphenyl tetrazolium bromide (MTT) colorimetric assay (Promega) per the manufacturer's instructions. Media was discarded, and firefly luciferase activity was measured (Promega) according to manufacturer's protocol. Light output was measured using a Spectramax L luminometer (Molecular Devices) with an

integration time of one second per well. Data was normalized to 100% of incremental BRE-Luc activity due to adenoviruses specifying caALK1, -2, or -3, or the incremental CAGA-Luc activity due to adenoviruses specifying caALK4 or -5. Graphing and regression analysis by sigmoidal dose−response with variable Hill coefficient was performed using GraphPad Prism software.

Cell Viability Assay. HepG2 hepatocarcinoma cells were seeded in DMEM supplemented with 10% FBS at 25000 cells per well in tissue culture treated 96-well plates (Costar 3610; Corning). The cells were incubated for 2 h (37 °C and 5% CO_2) and allowed to settle and attach. Compounds of interest or DMSO were diluted in DMEM and added at final compound concentrations of 1, 10, and 100 μM. Cells were incubated for 4 and 24 h, after which the media was discarded. Cells were lysed by adding 30 μL of passive lysis buffer (Promega) and shaken at RT for 15 min. Cell viability was determined by quantifying the ATP present in each well by adding 10 μL of Cell Titer Glo (Promega) per well and measuring the light output Spectramax L luminometer (Molecular Devices) with an integration time of one second per well. Data was normalized to 100% viability for cells receiving only DMSO without any concurrent compound.

■ ASSOCIATED CONTENT

Supporting Information

Additional data describing the cell-based activity of **15**, the correlation of IC_{50} and cytotoxicity, the docking model of **10**, diffraction data and refinement statistics, kinome selectivity data, and calculated physiochemical properties. This material is available free of charge via the Internet at http://pubs.acs.org.

Accession Codes

PDB ID code: 4BGG.

■ AUTHOR INFORMATION

Corresponding Authors

*For P.B.Y.: phone, 857-307-0390; E-mail, pbyu@partners.org.
*For G.D.C.: phone, 713-743-1274; E-mail, gdcuny@central.uh.edu.

Author Contributions

¶A.H.M. and Y.W. contributed equally. Compounds were conceived by A.H.M., Y.W., S.C., G.DC., and P.B.Y. Compounds were synthesized by Y.W., S.C., and X.X. Biological experiments were conceived and designed by A.H.M, C.E.S., A.N.B., G.DC., and P.B.Y. These experiments were conducted by A.H.M. Crystallography experiments were conducted by C.E.S. and P.C. The manuscript was written and revised by A.H.M., Y.W., C.E.S, A.N.B., G.D.C., and P.B.Y.

Notes

Brigham and Women's Hospital has applied for patents related to the use of these compounds for the treatment of FOP, DIPG and other disorders, and inventors (A.H.M., G.D.C., P.B.Y.) may be entitled to royalties. LDN-214117 will be available from Sigma-Aldrich (product SML1119) under a non-exclusive license for research use only.

■ ACKNOWLEDGMENTS

We thank the staff at the Diamond Light Source beamline I04-1 for help with diffraction data collection. This work was supported by grants from the U.S. National Institutes of Health DK082971-02S1 (A.H.M.), AR057374-03S1 (A.H.M.), HL079943, and AR057374 (P.B.Y.) and from the Pulmonary Hypertension Association (P.B.Y.), a Leducq Foundation Transatlantic Network of Excellence Award (P.B.Y.), a Howard Hughes Medical Institute Early Career Physician-Scientist Award (P.B.Y.), the Harvard NeuroDiscovery Center (Y.W., S.C., X.X., G.D.C.), FOP action UK (C.E.S.), FOP France (A.N.B.), and the Structural Genomics Consortium (A.N.B.). The SGC is a registered charity (number 1097737) that receives funds from AbbVie, Bayer PHARMA AG, Boehringer Ingelheim, the Canada Foundation for Innovation, the Canadian Institutes for Health Research, Genome Canada, GlaxoSmithKline, Janssen, Lilly Canada, the Novartis Research Foundation, the Ontario Ministry of Economic Development and Innovation, Pfizer, Takeda, and the Wellcome Trust [092809/Z/10/Z].

■ ABBREVIATIONS USED

BMP, bone morphogenetic protein; TGF-β, transforming growth factor β; FOP, fibrodysplasia ossificans progressiva

■ REFERENCES

(1) Kitisin, K.; Saha, T.; Blake, T.; Golestaneh, N.; Deng, M.; Kim, C.; Tang, Y.; Shetty, K.; Mishra, B.; Mishra, L. TGF-Beta Signaling in Development. *Sci. STKE* **2007**, *2007*, cm1.

(2) Waite, K. A.; Eng, C. From Developmental Disorder to Heritable Cancer: It's All in the BMP/TGF-Beta Family. *Nature Rev. Genet* **2003**, *4*, 763−773.

(3) Andriopoulos, B., Jr.; Corradini, E.; Xia, Y.; Faasse, S. A.; Chen, S.; Grgurevic, L.; Knutson, M. D.; Pietrangelo, A.; Vukicevic, S.; Lin, H. Y.; Babitt, J. L. BMP6 Is a Key Endogenous Regulator of Hepcidin Expression and Iron Metabolism. *Nature Genet.* **2009**, *41*, 482−487.

(4) Shi, Y.; Massague, J. Mechanisms of TGF-Beta Signaling from Cell Membrane to the Nucleus. *Cell* **2003**, *113*, 685−700.

(5) Schmierer, B.; Hill, C. S. TGFbeta−SMAD Signal Transduction: Molecular Specificity and Functional Flexibility. *Nature Rev. Mol. Cell Biol.* **2007**, *8*, 970−982.

(6) Chen, Y. G.; Hata, A.; Lo, R. S.; Wotton, D.; Shi, Y.; Pavletich, N.; Massague, J. Determinants of Specificity in TGF-Beta Signal Transduction. *Genes Dev.* **1998**, *12*, 2144−2152.

(7) Hong, C. C.; Yu, P. B. Applications of Small Molecule BMP Inhibitors in Physiology and Disease. *Cytokine Growth Factor Rev.* **2009**, *20*, 409−418.

(8) Kaplan, F. S.; Le Merrer, M.; Glaser, D. L.; Pignolo, R. J.; Goldsby, R. E.; Kitterman, J. A.; Groppe, J.; Shore, E. M. Fibrodysplasia Ossificans Progressiva. *Best Pract Res. Clin. Rheumatol.* **2008**, *22*, 191−205.

(9) Shore, E. M.; Xu, M.; Feldman, G. J.; Fenstermacher, D. A.; Brown, M. A.; Kaplan, F. S. A Recurrent Mutation in the BMP Type I Receptor Acvr1 Causes Inherited and Sporadic Fibrodysplasia Ossificans Progressiva. *Nature Genet.* **2006**, *38*, 525−527.

(10) Kaplan, F. S.; Xu, M.; Seemann, P.; Connor, J. M.; Glaser, D. L.; Carroll, L.; Delai, P.; Fastnacht-Urban, E.; Forman, S. J.; Gillessen-Kaesbach, G.; Hoover-Fong, J.; Koster, B.; Pauli, R. M.; Reardon, W.; Zaidi, S. A.; Zasloff, M.; Morhart, R.; Mundlos, S.; Groppe, J.; Shore, E. M. Classic and Atypical Fibrodysplasia Ossificans Progressiva (FOP) Phenotypes Are Caused by Mutations in the Bone Morphogenetic Protein (BMP) Type I Receptor Acvr1. *Hum. Mutat.* **2009**, *30*, 379−390.

(11) Petrie, K. A.; Lee, W. H.; Bullock, A. N.; Pointon, J. J.; Smith, R.; Russell, R. G.; Brown, M. A.; Wordsworth, B. P.; Triffitt, J. T. Novel Mutations in Acvr1 Result in Atypical Features in Two Fibrodysplasia Ossificans Progressiva Patients. *PLoS One* **2009**, *4*, e5005.

(12) Ohte, S.; Shin, M.; Sasanuma, H.; Yoneyama, K.; Akita, M.; Ikebuchi, K.; Jimi, E.; Maruki, Y.; Matsuoka, M.; Namba, A.; Tomoda, H.; Okazaki, Y.; Ohtake, A.; Oda, H.; Owan, I.; Yoda, T.; Furuya, H.; Kamizono, J.; Kitoh, H.; Nakashima, Y.; Susami, T.; Haga, N.; Komori, T.; Katagiri, T. A Novel Mutation of ALK2, L196p, Found in the Most Benign Case of Fibrodysplasia Ossificans Progressiva Activates BMP-Specific Intracellular Signaling Equivalent to a Typical Mutation, R206h. *Biochem. Biophys. Res. Commun.* **2011**, *407*, 213−218.

(13) Gregson, C. L.; Hollingworth, P.; Williams, M.; Petrie, K. A.; Bullock, A. N.; Brown, M. A.; Tobias, J. H.; Triffitt, J. T. A Novel Acvr1 Mutation in the Glycine/Serine-Rich Domain Found in the

Most Benign Case of a Fibrodysplasia Ossificans Progressiva Variant Reported to Date. *Bone* **2011**, *48*, 654−658.
(14) Fukuda, T.; Kanomata, K.; Nojima, J.; Kokabu, S.; Akita, M.; Ikebuchi, K.; Jimi, E.; Komori, T.; Maruki, Y.; Matsuoka, M.; Miyazono, K.; Nakayama, K.; Nanba, A.; Tomoda, H.; Okazaki, Y.; Ohtake, A.; Oda, H.; Owan, I.; Yoda, T.; Haga, N.; Furuya, H.; Katagiri, T. A Unique Mutation of ALK2, G356d, Found in a Patient with Fibrodysplasia Ossificans Progressiva Is a Moderately Activated BMP Type I Receptor. *Biochem. Biophys. Res. Commun.* **2008**, *377*, 905−909.
(15) Wu, G.; Diaz, A. K.; Paugh, B. S.; Rankin, S. L.; Ju, B.; Li, Y.; Zhu, X.; Qu, C.; Chen, X.; Zhang, J.; Easton, J.; Edmonson, M.; Ma, X.; Lu, C.; Nagahawatte, P.; Hedlund, E.; Rusch, M.; Pounds, S.; Lin, T.; Onar-Thomas, A.; Huether, R.; Kriwacki, R.; Parker, M.; Gupta, P.; Becksfort, J.; Wei, L.; Mulder, H. L.; Boggs, K.; Vadodaria, B.; Yergeau, D.; Russell, J. C.; Ochoa, K.; Fulton, R. S.; Fulton, L. L.; Jones, C.; Boop, F. A.; Broniscer, A.; Wetmore, C.; Gajjar, A.; Ding, L.; Mardis, E. R.; Wilson, R. K.; Taylor, M. R.; Downing, J. R.; Ellison, D. W.; Baker, S. J. The Genomic Landscape of Diffuse Intrinsic Pontine Glioma and Pediatric Non-Brainstem High-Grade Glioma. *Nature Genet.* **2014**, *46*, 444−450.
(16) Fontebasso, A. M.; Papillon-Cavanagh, S.; Schwartzentruber, J.; Nikbakht, H.; Gerges, N.; Fiset, P. O.; Bechet, D.; Faury, D.; De Jay, N.; Ramkissoon, L. A.; Corcoran, A.; Jones, D. T.; Sturm, D.; Johann, P.; Tomita, T.; Goldman, S.; Nagib, M.; Bendel, A.; Goumnerova, L.; Bowers, D. C.; Leonard, J. R.; Rubin, J. B.; Alden, T.; Browd, S.; Geyer, J. R.; Leary, S.; Jallo, G.; Cohen, K.; Gupta, N.; Prados, M. D.; Carret, A. S.; Ellezam, B.; Crevier, L.; Klekner, A.; Bognar, L.; Hauser, P.; Garami, M.; Myseros, J.; Dong, Z.; Siegel, P. M.; Malkin, H.; Ligon, A. H.; Albrecht, S.; Pfister, S. M.; Ligon, K. L.; Majewski, J.; Jabado, N.; Kieran, M. W. Recurrent Somatic Mutations in Acvr1 in Pediatric Midline High-Grade Astrocytoma. *Nature Genet.* **2014**, *46*, 462−466.
(17) Taylor, K. R.; Mackay, A.; Truffaux, N.; Butterfield, Y. S.; Morozova, O.; Philippe, C.; Castel, D.; Grasso, C. S.; Vinci, M.; Carvalho, D.; Carcaboso, A. M.; de Torres, C.; Cruz, O.; Mora, J.; Entz-Werle, N.; Ingram, W. J.; Monje, M.; Hargrave, D.; Bullock, A. N.; Puget, S.; Yip, S.; Jones, C.; Grill, J. Recurrent Activating Acvr1 Mutations in Diffuse Intrinsic Pontine Glioma. *Nature Genet.* **2014**, *46*, 457−461.
(18) Buczkowicz, P.; Hoeman, C.; Rakopoulos, P.; Pajovic, S.; Letourneau, L.; Dzamba, M.; Morrison, A.; Lewis, P.; Bouffet, E.; Bartels, U.; Zuccaro, J.; Agnihotri, S.; Ryall, S.; Barszczyk, M.; Chornenkyy, Y.; Bourgey, M.; Bourque, G.; Montpetit, A.; Cordero, F.; Castelo-Branco, P.; Mangerel, J.; Tabori, U.; Ho, K. C.; Huang, A.; Taylor, K. R.; Mackay, A.; Bendel, A. E.; Nazarian, J.; Fangusaro, J. R.; Karajannis, M. A.; Zagzag, D.; Foreman, N. K.; Donson, A.; Hegert, J. V.; Smith, A.; Chan, J.; Lafay-Cousin, L.; Dunn, S.; Hukin, J.; Dunham, C.; Scheinemann, K.; Michaud, J.; Zelcer, S.; Ramsay, D.; Cain, J.; Brennan, C.; Souweidane, M. M.; Jones, C.; Allis, C. D.; Brudno, M.; Becher, O.; Hawkins, C. Genomic Analysis of Diffuse Intrinsic Pontine Gliomas Identifies Three Molecular Subgroups and Recurrent Activating Acvr1 Mutations. *Nature Genet.* **2014**, *46*, 451−456.
(19) Cuny, G. D.; Yu, P. B.; Laha, J. K.; Xing, X.; Liu, J. F.; Lai, C. S.; Deng, D. Y.; Sachidanandan, C.; Bloch, K. D.; Peterson, R. T. Structure−Activity Relationship Study of Bone Morphogenetic Protein (BMP) Signaling Inhibitors. *Bioorg. Med. Chem. Lett.* **2008**, *18*, 4388−4392.
(20) Hao, J.; Ho, J. N.; Lewis, J. A.; Karim, K. A.; Daniels, R. N.; Gentry, P. R.; Hopkins, C. R.; Lindsley, C. W.; Hong, C. C. In Vivo Structure−Activity Relationship Study of Dorsomorphin Analogues Identifies Selective Vegf and BMP Inhibitors. *ACS Chem. Biol.* **2009**, *5*, 245−253.
(21) Mohedas, A. H.; Xing, X.; Armstrong, K. A.; Bullock, A. N.; Cuny, G. D.; Yu, P. B. Development of an ALK2-Biased BMP Type I Receptor Kinase Inhibitor. *ACS Chem. Biol.* **2013**, *8*, 1291−1302.
(22) Yu, P. B.; Deng, D. Y.; Lai, C. S.; Hong, C. C.; Cuny, G. D.; Bouxsein, M. L.; Hong, D. W.; McManus, P. M.; Katagiri, T.; Sachidanandan, C.; Kamiya, N.; Fukuda, T.; Mishina, Y.; Peterson, R. T.; Bloch, K. D. BMP Type I Receptor Inhibition Reduces Heterotopic Ossification. *Nature Med.* **2008**, *14*, 1363−1369.
(23) Sanvitale, C. E.; Kerr, G.; Chaikuad, A.; Ramel, M. C.; Mohedas, A. H.; Reichert, S.; Wang, Y.; Triffitt, J. T.; Cuny, G. D.; Yu, P. B.; Hill, C. S.; Bullock, A. N. A New Class of Small Molecule Inhibitor of BMP Signaling. *PLoS One* **2013**, *8*, e62721.
(24) Cui, J. J.; Tran-Dube, M.; Shen, H.; Nambu, M.; Kung, P. P.; Pairish, M.; Jia, L.; Meng, J.; Funk, L.; Botrous, I.; McTigue, M.; Grodsky, N.; Ryan, K.; Padrique, E.; Alton, G.; Timofeevski, S.; Yamazaki, S.; Li, Q.; Zou, H.; Christensen, J.; Mroczkowski, B.; Bender, S.; Kania, R. S.; Edwards, M. P. Structure Based Drug Design of Crizotinib (Pf-02341066), a Potent and Selective Dual Inhibitor of Mesenchymal−Epithelial Transition Factor (C-Met) Kinase and Anaplastic Lymphoma Kinase (ALK). *J. Med. Chem.* **2011**, *54*, 6342−6363.
(25) Miyaura, N.; Yanagi, T.; Suzuki, A. The Palladium-Catalyzed Cross-Coupling Reaction of Phenylboronic Acid with Haloarenes in the Presence of Bases. *Synth. Commun.* **1981**, *11*, 513−519.
(26) Alo, B. I.; Kandil, A.; Patil, P. A.; Sharp, M. J.; Siddiqui, M. A.; Snieckus, V.; Josephy, P. D. Sequential Directed Ortho Metalation−Boronic Acid Cross-Coupling Reactions. A General Regiospecific Route to Oxygenated Dibenzo[*b*,*d*]pyran-6-ones Related to Ellagic Acid. *J. Org. Chem.* **1991**, *56*, 3763−3768.
(27) Hilton, S.; Naud, S.; Caldwell, J. J.; Boxall, K.; Burns, S.; Anderson, V. E.; Antoni, L.; Allen, C. E.; Pearl, L. H.; Oliver, A. W.; Aherne, G. W.; Garrett, M. D.; Collins, I. Identification and Characterisation of 2-Aminopyridine Inhibitors of Checkpoint Kinase 2 (Vol 18, Pg 707, 2010). *Bioorg. Med. Chem.* **2010**, *18*, 4591−4591.
(28) Gray, M.; Andrews, I. P.; Hook, D. F.; Kitteringham, J.; Voyle, M. Practical Methylation of Aryl Halides by Suzuki−Miyaura Coupling. *Tetrahedron Lett.* **2000**, *41*, 6237−6240.
(29) Lipinski, C. A.; Lombardo, F.; Dominy, B. W.; Feeney, P. J. Experimental and Computational Approaches to Estimate Solubility and Permeability in Drug Discovery and Development Settings. *Adv. Drug Delivery Rev.* **2001**, *46*, 3−26.
(30) Veber, D. F.; Johnson, S. R.; Cheng, H. Y.; Smith, B. R.; Ward, K. W.; Kopple, K. D. Molecular Properties That Influence the Oral Bioavailability of Drug Candidates. *J. Med. Chem.* **2002**, *45*, 2615−2623.
(31) Fedorov, O.; Marsden, B.; Pogacic, V.; Rellos, P.; Muller, S.; Bullock, A. N.; Schwaller, J.; Sundstrom, M.; Knapp, S. A Systematic Interaction Map of Validated Kinase Inhibitors with Ser/Thr Kinases. *Proc. Natl. Acad. Sci. U. S. A.* **2007**, *104*, 20523−20528.
(32) Luo, J.; Tang, M.; Huang, J.; He, B. C.; Gao, J. L.; Chen, L.; Zuo, G. W.; Zhang, W.; Luo, Q.; Shi, Q.; Zhang, B. Q.; Bi, Y.; Luo, X.; Jiang, W.; Su, Y.; Shen, J.; Kim, S. H.; Huang, E.; Gao, Y.; Zhou, J. Z.; Yang, K.; Luu, H. H.; Pan, X.; Haydon, R. C.; Deng, Z. L.; He, T. C. TGFbeta/BMP Type I Receptors ALK1 and ALK2 Are Essential for BMP9-Induced Osteogenic Signaling in Mesenchymal Stem Cells. *J. Biol. Chem.* **2010**, *285*, 29588−29598.
(33) Ramsden, N.; Wilson, F. *Aminopyridine Derivates as Kinase Inhibitors*. Patent WO2008025820 A1, 2008.
(34) Blackaby, W. P.; Charles, M. D.; Ekwuru, C. T.; Foxton, C. H.; Hammonds, T. R.; Pave, G. A.; Raynham, T. M.; Stevens, A. P. *Pyridine Benzamides and Pyrazine Benzamides Used as Pkd Inhibitors*. Patent WO2008025820 A1, 2008.
(35) Yu, P. B.; Beppu, H.; Kawai, N.; Li, E.; Bloch, K. D. Bone Morphogenetic Protein (BMP) Type II Receptor Deletion Reveals BMP Ligand-Specific Gain of Signaling in Pulmonary Artery Smooth Muscle Cells. *J. Biol. Chem.* **2005**, *280*, 24443−24450.
(36) Aoki, H.; Fujii, M.; Imamura, T.; Yagi, K.; Takehara, K.; Kato, M.; Miyazono, K. Synergistic Effects of Different Bone Morphogenetic Protein Type I Receptors on Alkaline Phosphatase Induction. *J. Cell Sci.* **2001**, *114*, 1483−1489.
(37) Nakajima, M.; Haga, N.; Takikawa, K.; Manabe, N.; Nishimura, G.; Ikegawa, S. The Acvr1 617g>a Mutation Is Also Recurrent in Three Japanese Patients with Fibrodysplasia Ossificans Progressiva. *J. Hum. Genet.* **2007**, *52*, 473−475.

(38) Bocciardi, R.; Bordo, D.; Di Duca, M.; Di Rocco, M.; Ravazzolo, R. Mutational Analysis of the Acvr1 Gene in Italian Patients Affected with Fibrodysplasia Ossificans Progressiva: Confirmations and Advancements. *Eur. J. Hum. Genet.* **2009**, *17*, 311−318.
(39) Lee, D. Y.; Cho, T. J.; Lee, H. R.; Park, M. S.; Yoo, W. J.; Chung, C. Y.; Choi, I. H. Acvr1 Gene Mutation in Sporadic Korean Patients with Fibrodysplasia Ossificans Progressiva. *J. Korean Med. Sci.* **2009**, *24*, 433−437.
(40) Chaikuad, A.; Alfano, I.; Kerr, G.; Sanvitale, C. E.; Boergermann, J. H.; Triffitt, J. T.; von Delft, F.; Knapp, S.; Knaus, P.; Bullock, A. N. Structure of the BMP Receptor ALK2 and Implications for Fibrodysplasia Ossificans Progressiva. *J. Biol. Chem.* **2012**, *287*, 36990−36998.
(41) Bagarova, J.; Vonner, A. J.; Armstrong, K. A.; Borgermann, J.; Lai, C. S.; Deng, D. Y.; Beppu, H.; Alfano, I.; Filippakopoulos, P.; Morrell, N. W.; Bullock, A. N.; Knaus, P.; Mishina, Y.; Yu, P. B. Constitutively Active ALK2 Receptor Mutants Require Type II Receptor Cooperation. *Mol. Cell. Biol.* **2013**, *33*, 2413−2424.
(42) Miller, D. S.; Horowitz, S. B. Intracellular Compartmentalization of Adenosine Triphosphate. *J. Biol. Chem.* **1986**, *261*, 13911−13915.
(43) Issa, A. M.; Phillips, K. A.; Van Bebber, S.; Nidamarthy, H. G.; Lasser, K. E.; Haas, J. S.; Alldredge, B. K.; Wachter, R. M.; Bates, D. W. Drug Withdrawals in the United States: A Systematic Review of the Evidence and Analysis of Trends. *Curr. Drug Saf.* **2007**, *2*, 177−185.
(44) Niesen, F. H.; Berglund, H.; Vedadi, M. The Use of Differential Scanning Fluorimetry to Detect Ligand Interactions That Promote Protein Stability. *Nature Protoc.* **2007**, *2*, 2212−2221.
(45) Leslie, A. G. The Integration of Macromolecular Diffraction Data. *Acta Crystallogr., Sect. D: Biol. Crystallogr.* **2006**, *62*, 48−57.
(46) McCoy, A. J.; Grosse-Kunstleve, R. W.; Adams, P. D.; Winn, M. D.; Storoni, L. C.; Read, R. J. Phaser Crystallographic Software. *J. Appl. Crystallogr.* **2007**, *40*, 658−674.
(47) Emsley, P.; Lohkamp, B.; Scott, W. G.; Cowtan, K. Features and Development of Coot. *Acta Crystallogr., Sect. D: Biol. Crystallogr.* **2010**, *66*, 486−501.
(48) Murshudov, G. N.; Vagin, A. A.; Dodson, E. J. Refinement of Macromolecular Structures by the Maximum-Likelihood Method. *Acta Crystallogr., Sect. D: Biol. Crystallogr.* **1997**, *53*, 240−255.
(49) Painter, J.; Merritt, E. A. Optimal Description of a Protein Structure in Terms of Multiple Groups Undergoing Tls Motion. *Acta Crystallogr., Sect. D: Biol. Crystallogr.* **2006**, *62*, 439−450.
(50) Davis, I. W.; Leaver-Fay, A.; Chen, V. B.; Block, J. N.; Kapral, G. J.; Wang, X.; Murray, L. W.; Arendall, W. B., III; Snoeyink, J.; Richardson, J. S.; Richardson, D. C. Molprobity: All-Atom Contacts and Structure Validation for Proteins and Nucleic Acids. *Nucleic Acids Res.* **2007**, *35*, W375−383.
(51) Adams, P. D.; Afonine, P. V.; Bunkoczi, G.; Chen, V. B.; Davis, I. W.; Echols, N.; Headd, J. J.; Hung, L. W.; Kapral, G. J.; Grosse-Kunstleve, R. W.; McCoy, A. J.; Moriarty, N. W.; Oeffner, R.; Read, R. J.; Richardson, D. C.; Richardson, J. S.; Terwilliger, T. C.; Zwart, P. H. Phenix: A Comprehensive Python-Based System for Macromolecular Structure Solution. *Acta Crystallogr., Sect. D: Biol. Crystallogr.* **2010**, *66*, 213−221.
(52) Zilberberg, L.; ten Dijke, P.; Sakai, L. Y.; Rifkin, D. B. A Rapid and Sensitive Bioassay to Measure Bone Morphogenetic Protein Activity. *BMC Cell Biol.* **2007**, *8*, 41−50.
(53) Oida, T.; Weiner, H. L. Murine Cd4 T Cells Produce a New Form of TGF-Beta as Measured by a Newly Developed TGF-Beta Bioassay. *PloS One* **2011**, *6*, e18365.
(54) Laskowski, R. A.; Swindells, M. B. Ligplot+: Multiple Ligand−Protein Interaction Diagrams for Drug Discovery. *J. Chem. Inf Model.* **2011**, *51*, 2778−2786.